



MARMARA UNIVERSITY
INSTITUTE OF SCIENCES



**SYNTHESIS AND CHARACTERIZATION
OF THE INULIN- POLY (ϵ -CAPROLACTONE)
COPOLYMER FOR USE IN DRUG
DELIVERY SYSTEM**

KÜBRA AYTEKİN

MASTER THESIS

Department of Chemical Engineering

Thesis Supervisor

Prof. Dr. MEHMET SAYIP EROĞLU

Thesis CO-Supervisor

Assist. Prof. Dr. MÜGE SENNAROĞLU BOSTAN

İSTANBUL, 2023



MARMARA UNIVERSITY
INSTITUTE OF SCIENCES



**SYNTHESIS AND CHARACTERIZATION
OF THE INULIN- POLY (ϵ -CAPROLACTONE)
COPOLYMER FOR USE IN DRUG
DELIVERY SYSTEM**

KÜBRA AYTEKİN

(524517017)

MASTER THESIS

Department of Chemical Engineering

Thesis Supervisor

Prof. Dr. MEHMET SAYIP EROĞLU

Thesis CO-Supervisor

Assist. Prof. Dr. MÜGE SENNAROĞLU BOSTAN

İSTANBUL, 2023

ACKNOWLEDGEMENT

First of all, I want to express my deepest thanks to my advisor Prof. Dr. Mehmet Sayıp EROĞLU for his guidance, patience, support, and motivation throughout my thesis. I would like to emphasize my sincere gratitude to my co-advisor Assist. Prof. Dr. Müge SENNAROĞLU BOSTON for her help. I would also like to thank Dr. Mural ÜNAL for his continuous support, immense knowledge, and extremely valuable advice. Their motivations have a huge effect on the success of this thesis.

I sincerely thank Assist Prof. Fatemeh BAHADORI for their interest and contributions. I also thank Assoc. Prof. Dr. Neslihan ALEMDAR YAYLA, and Res. Assist. Didem AYCAN, because of necessary equipment and the permission of using UV spectrophotometry.

Finally, I would especially like to thank my dear mother Nezihe İŞCAN, and my dear late father Cemil İŞCAN for their efforts and support throughout my whole life, and endless love. Also, special thanks to my husband Yunus AYTEKİN for his encouragement and his support.

May, 2023

Kübra AYTEKİN

TABLE OF CONTENTS	PAGE
ACKNOWLEDGEMENT.....	iii
ÖZET	vii
ABSTRACT	viii
CLAIM FOR ORIGINALITY	ix
SYMBOLS	x
ABBREVIATIONS	xii
LIST OF FIGURES.....	xiv
LIST OF TABLES	xvi
1. INTRODUCTION	1
1.1. Aim of the Study	1
1.2. Inulin.....	1
1.2.1. Chemical structure and physicochemical properties	1
1.2.2. Applications of inulin	2
1.3. Inulin-Based Copolymers	4
1.4. Poly (ϵ -caprolactone)(PCL).....	4
1.4.1. Chemical structure and physicochemical properties	5
1.4.2. Applications of poly (ϵ -caprolactone)(PCL)	6
1.5. Poly (ϵ -caprolactone)(PCL) Based Copolymers	7
1.6. The Microwave Technology.....	8
1.7. Coupling Reaction	9
1.8. Copolymers for Drug Delivery System	10
1.8.1. Nanoparticle (NP)-based drug delivery system.....	10
1.8.1.1. Self-assembly method.....	11
1.9. Mesalazine (mesalamine, 5-Aminosalicylic acid, 5-ASA)	13

2. MATERIALS AND METHODS	14
2.1. Materials	14
2.2. Equipments	14
2.2.1. Microwave oven	14
2.2.2. Gel permeation chromatography-Light scattering (GPC-LS)	14
2.2.3. Fourier transform infrared spectroscopy (FT-IR).....	15
2.2.4. Nuclear magnetic resonance spectroscopy (NMR)	15
2.2.5. Homogenizer	15
2.2.6. Dynamic light scattering (DLS)	15
2.2.7. Lyophilizer	16
2.2.8. Scanning electron microscope (SEM)	16
2.2.9. Shaking incubator	16
2.2.10. Ultraviolet-visible (UV-VIS) spectrophotometer	16
2.2.11. Differential scanning calorimetry (DSC)	16
2.2.12. Vacuum drying oven	17
2.3. Methods	17
2.3.1. Microwave-assisted ring opening polymerization of ϵ -caprolactone.....	17
2.3.2. Synthesis of PCL grafted inulin copolymer (In-g-PCL)	18
2.3.3. Drug loading process and release studies	19
2.3.3.1. Preparation of Nano/microemulsion and Drug Loading	19
2.3.3.2. Drug release studies.....	20
3. RESULTS AND DISCUSSION.....	23
3.1. Spectroscopic Characterization	23
3.1.1. FTIR Analysis	23
3.1.2. NMR Analysis	25

3.2. Differential Scanning Calorimetry (DSC) Analysis.....	28
3.3. SEM Analysis.....	29
3.4. Particle Size Distribution and Zeta Potential.....	31
3.5. Drug Release Studies.....	33
4. CONCLUSION	36
REFERENCES	37

ÖZET

İLAC SALIM SISTEMİNDE KULLANIM İÇİN INULİN-POLİ(ε-KAPROLAKTON) KOPOLİMERİNİN SENTEZİ VE KARAKTERİZASYONU

İlaç salınımı alanında, ilacın biyoyumlu olması ve diğer organlara zarar vermeden tedavi edilecek hücrelere ulaşması önemlidir. Bu çalışmada, i) biyoyumlu, ii) biyobozunur, iii) uygun ilaç maddesini taşıyabilme kapasitesine sahip bir kopolimer sentezlenmesi amaçlanmıştır.

İnülin (In), $\beta(2\rightarrow1)$ glikosidik bağlarla bağlanan fruktoz birimlerinden oluşan ve tipik olarak terminal glikoz gruplarına sahip bir polisakkarittir. Kalın bağırsakta enzimatik olarak emilir ve sindirilir. İnsan dokusuna uyum sağlaması, esnek ve biyolojik olarak parçalanabilir yapısı inulinin öne çıkan özellikleridir.

Polikaprolakton (PCL), yavaş biyobozunurluğu ve düşük moleküler ağırlığı nedeniyle kontrollü ilaç salımında hidrofobik bir çekirdek olarak kullanılır. Böylece, In'ın PCL ile kopolimerizasyonu, ilaç taşıyıcı olarak kullanım kapasitesini artırır ve ilaç formülasyonunun ana bileşenini oluşturur.

Bu çalışmada PCL, ϵ -kaprolakton'un (ϵ -CL) "mikrodalga yardımı ile halka açılımı reaksiyonu" (ROP), tekniği kullanılarak polimerizasyonu ile sentezlenmiştir ve bu çalışmada asetik asit başlatıcı olarak kullanılmıştır. Sentezlenen düşük molekül ağırlıklı ve karboksilik asit uç gruplu PCL-COOH "dicyclohexyl carbodiimide (DCC) coupling" reaksiyonu kullanılarak In üzerine aşılantılmıştır. Sentezlenen PCL aşılı inulin kopolimeri (In-g-PCL) emülsiyeye edilmiş ve bundan hazırlanan nano/mikro misel yapısındaki partiküllere 5-ASA yüklenerek bunların ilaç salım profili incelenmiştir.

Sentezlenen PCL-COOH ve In-g-PCL kopolimeri diferansiyel taramalı termal analiz (DSC), nükleer manyetik rezonans (NMR), Fourier transform infrared (FT-IR) teknikleri ile detaylı karakterizasyonu yapılmıştır. Hazırlanan nano/mikro yapı parçacıkların ilaçsız ve ilaçlı olarak taramalı elektron mikroskopu (SEM) ile görüntüsü alınarak PBS (ph 7.4) içinde UV-VIS spektroskopisi ile salım çalışmaları yapılmıştır. Salım çalışmalarının istatistiksel analizi yapılmıştır.

ABSTRACT

SYNTHESIS AND CHARACTERIZATION OF INULIN- POLY(ϵ -CAPROLACTONE) COPOLYMER FOR USE IN DRUG DELIVERY SYSTEMS.

In the field of drug delivery, it is important that the drug carrier system should be biocompatible and reaches the cells to be treated without damaging other organs. This study aimed to synthesize a copolymer that is i) biocompatible, ii) biodegradable, iii) capable of carrying the appropriate drug substance.

Inulin (In) is a polysaccharide composed of fructose units linked by $\beta(2\rightarrow1)$ glycosidic bonds and typically with terminal glucose groups. This polysaccharide is enzymatically absorbed in the large intestine and digested. Adaptation to human tissue, flexible structure and biodegradability are the prominent features of inulin.

Polycaprolactone (PCL) is widely used as the core in drug-carrying formulations due to its slow biodegradability and hydrophobicity. Due to the aforementioned properties of these polymers copolymer of inulin with PCL provides remarkable advantages in the preparation of nano drug formulations.

In this study, PCL was synthesized by the microwave assisted ring opening polymerization of ϵ -caprolactone using acetic acid as initiator and grafted onto inulin via the DCC coupling reaction. Therefore, the synthesized In-g-PCL was emulsified, 5-ASA was loaded on the prepared nano/micro micelles and their drug release behavior was investigated.

Detailed characterization of the synthesized carboxylic acid terminated PCL (PCL-COOH) and In-g-PCL copolymers were performed using DSC, NMR, and FT-IR techniques. The SEM images of the prepared nano/micro-structured micellar particles with and without drug were obtained and the release studies were performed in PBS (pH 7.4) by UV-VIS spectroscopy. The statistical analyses of the release behavior of the particles were also studied.

CLAIM FOR ORIGINALITY

The subject of this thesis is original and there are no research studies on the synthesis of PCL grafted inulin copolymer (In-g-PCL) and its application as a controlled drug carrier. Due to the quite different thermodynamic behavior of PCL and inulin, In-g-PCL could be synthesized as a result of many repeated synthesis studies. For this reason, the difficulties were encountered in finding common solvents in NMR characterization studies and evaluating the chemical structure. Therefore, the thesis presented by me is the product of my independent and original works. This thesis does not contain any plagiarism and was not submitted for publication before.

SYMBOLS

G	: Glucose unit
F	: Fructose unit
N	: The number of fructose units
m	: The number of fructose units
°C	: Celsius degree
%	: Percentage
h	: Hour
cm⁻¹	: reciprocal centimeter (or wavenumber)
nm	: nanometer
g/l	: Gram/liter
g/mole	: Gram/mole
mg	: milligram
mL	: milliliter
ppm	: Parts Per Million
R²	: Standard deviation, Correlation coefficient
mV	: Milivolt
Rpm	: Revolutions per minute
MHz	: Megahertz
V	: Volume
v	: Volume of micelle solution
µm	: micrometer
mPa.s	: milipascal second
Mn	: Number average molecular weight

T_g : Glass transition temperature
C : Concentration
M_i : Initial weight
m : Weight of the measured drug
m_i : Initial weight of drug within the micelles
Sn(Oct)₂ : Stannous octanoate

ABBREVIATIONS

PCL	: Poly(ϵ -caprolactone)
DP	: Degree of polymerization
DMF	: Dimetilformamide
ROP	: Ring-opening polymerization
NP	: Nanoparticle
IBD	: Inflammatory bowel disease
5-ASA	: 5-Aminosalicylic Acid (Mesalazine)
DLS	: Dynamic Light Scattering
NMR	: Nuclear Magnetic Resonance
PBS	: Phosphate Buffered Saline
DMSO	: Dimethyl sulfoxide
GIS	: Gastrointestinal system
CMC	: Critical micelle concentration
EPR	: Enhance permeability and retention
INU	: Inulin
PLA	: Poly(lactic acid)
PEG	: Polyethylene glycol
INU-EDAP	: Inulin-pentyne
C-DOXO	: Citraconic-doxorubicin
DCC	: N, N'-Dicyclohexylcarbodiimide
NHS	: N-hydroxysuccinimide
THF	: Tetrahydrofuran
GPC-LS	: Gel permeation chromatography-light scattering
FTIR	: Fourier transform infrared

PCS : Photon Correlation Spectroscopy

SEM : Scanning electron microscope

UV-VIS : Ultraviolet-visible

DSC : Differential scanning calorimetry

In-g-PCL : PCL grafted inulin

LIST OF FIGURES	PAGE
Figure 1. Molecular structure of inulin (GF _n , F _m)	1
Figure 2. Polycondensation of 6-hydroxycaproic acid during PCL synthesis.....	5
Figure 3. Ring-opening polymerization of ϵ -caprolactone	5
Figure 4. The structure of caprolactone and PCL.....	6
Figure 5. DCC coupling reaction mechanism	9
Figure 6. Micelle formation for an amphiphilic copolymer	12
Figure 7. The chemical structure of 5-ASA	13
Figure 8. The synthesis of Polycaprolactone (PCL).....	17
Figure 9. Synthesis mechanism of Inulin-PCL copolymer.....	19
Figure 10. 5-ASA absorbance-concentration calibration curve	20
Figure 11. % Released of 5-ASA versus time graph.....	21
Figure 12. 5-ASA absorbance-concentration calibration curve in 1.5:2 PBS:DMF	22
Figure 13. FTIR spectrum of PCL.....	23
Figure 14. FT-IR spectrum of inulin.....	24
Figure 15. FTIR spectrum of In-g-PCL.....	25
Figure 16. ¹ H NMR spectrum of PCL	26
Figure 17. ¹ H-NMR spectrum of inulin.....	27
Figure 18. ¹ H-NMR spectrum of copolymer (In-g-PCL)	28
Figure 19. DSC thermogram of In-g-PCL.....	29
Figure 20. SEM image of the In-g-PCL particles before 5-ASA loading	30

Figure 21. SEM images of the 5-ASA loaded In-g-PCL copolymer particles at a)20.000 b)6.000 c)4.000 magnifications.	31
Figure 22. Particle size distribution of the 5-ASA unloaded In-g-PCL micelles.	32
Figure 23. Particle size distribution of the 5-ASA loaded In-g-PCL micelles.	32
Figure 24. Release profile of 5-ASA from the In-g-PCL micelles.	33
Figure 25. Zero Order Model.....	34
Figure 26. First Order Model.....	34
Figure 27. Korsmeyer-Peppas Model	35
Figure 28. Hixson-Crowell Model.....	35

LIST OF TABLES

PAGE

Table 1. The physico-chemical properties of inulin 2

Table 2. The properties of 5-ASA 14

1. INTRODUCTION

1.1. Aim of the Study

The aim of this thesis was firstly the synthesis of the amphiphilic inulin-g-poly (ϵ -caprolactone) (In-g-PCL) copolymer, secondly the preparation of nano/micro micellar drug carriers from the synthesized copolymer, and finally the spectroscopic, chemical, and physicochemical characterization of the particles prepared from the synthesized copolymer and statistical analyses of their drug release profile.

1.2. Inulin

Valantine Rose, a German scientist, first discovered inulin in 1804 when she extracted it from the roots of *Inula helenium* with boiling water. This carbohydrate was named inulin by Thomson [1, 2].

Inulin occurs abundantly in nature in fungi, some bacteria, and especially in plants such as chicory, onion, garlic, leek, banana, dandelion, wheat, asparagus, dahlia, rye, Jerusalem artichoke, and yacon. Inulin is used in the food and pharmaceutical industries [3].

1.2.1. Chemical structure and physicochemical properties

Inulin is a type of fructan polymer composed of D-fructose with β -(2 \rightarrow 1)-bonds (Fm) and terminal D-glucose with α -(1 \rightarrow 2) bonds (GFn). Molecular structure of inulin was presented in Figure 1.

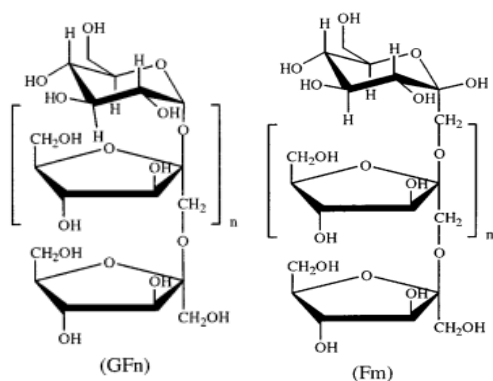


Figure 1. Molecular structure of inulin (GFn, Fm) [9]

According to the literature, inulin is water soluble, biodegradable and biocompatible, nontoxic with a flexible structure, and quite stabilizing with protective effects [1]. These properties of inulin make it a suitable polymer for the preparation of drug carriers made from its copolymers with various biocompatible polymers for use in the human body.

GF_n and F_m in Figure 1 are the separations of inulin. G represents the glucose unit, F represents the fructose unit, n and m represent the number of fructose units [4]. The degree of polymerization (DP) of inulin varies from 2 to 70 depending on the type of plant, age of the plant, and weather conditions during growth [9]. The formula of inulin is C_{6n}H_{10n+2}O_{5n+1}, and its molecular weight is in the range of 3-8 kDa, which varies depending on the plant source [5]. The physicochemical properties of inulin are listed in Table 1.

Table 1. The physico-chemical properties of inulin [3]

	Standard Inulin
Chemical structure	GF _n (2 ≤ n ≤ 60)
Average degree of polymerization	12
PH(10% w/w)	5-7
Appearance	White Powder
Taste	Neutral
Solubility in water at 25 °C (g/L)	120
Viscosity in water (5%) at 10 °C (mPa.s)	1.6
Sulphated ash (% on d.m.)	<0.2
Heavy metals (ppm on d.m.)	<0.2

Hilman et. al., (2018) determined the immunomodulatory effects and increased mineral absorption of inulin during fermentation [5].

1.2.2. Applications of inulin

A prebiotic is a substance that selectively acts on the host by increasing the growth and

activity of certain indigenous bacteria, thus improving the health of the host as an indigestible substance [2]. Van Loo et al., (1999) stated that the consequences of research in the presence of β -(2 \rightarrow 1)-type fructans are prebiotic. Therefore, inulin is also prebiotic.

Prebiotics can cause certain changes in the composition and activity of gastrointestinal microflora (Bifidobacteria and Lactobacilli). These prebiotics are associated with health benefits such as greater stimulation of immune functions, improved gut microbiota, lower risks of irritable bowel disease and constipation, and better mineral absorption. They also reduce the risk of colorectal cancer and cholesterol [2, 6]. These properties are useful to assist the pharmaceutical industry in the development of drug delivery systems.

In addition, cancer cells have higher energy requirements than normal cells. The main energy sources of cells are polysaccharides. Therefore, polysaccharides are main energy sources for cancer cells. Moreover, they have a high ability to adhere to cancer cells. They interact with carbohydrate-binding proteins on the cell surface and also enhance permeability and retention (EPR) [36, 37, 38]. For this reason, nano/micro-particles consisting of a hydrophilic polysaccharide surface and a hydrophobic inner core are suitable nanocarriers for targeted drug delivery in cancer and cancer cell imaging systems.

Inulin occurs in natural carbohydrates as non-digestible oligosaccharides. When thinking of inulin in the human body, it is absorbable in the small intestine due to the β -configuration of C-2. However, the intestinal microflora in the colon can ferment inulin [7]. This property makes it a perfect choice for a colon-targeted drug system. Inulin can be used to improve the poor dissolution of poorly soluble drugs, modulate lipid production, treat constipation, as a vaccine adjuvant, measure renal function, control blood glucose levels, as a dietary fiber, as a prebiotic, prevent or alleviate the symptoms of intestinal diseases [8], and to treat cancer [6]. In addition, inulin and its derivatives have been used in the food and pharmaceutical industries, and water treatment [24].

Hydrogels, micelles, nanoparticles, microparticles, solid dispersions, liposomes, and conjugates are the types of carriers in drug delivery systems. These carriers can be formed by modification of inulin. In this study, micro/nano-particles were used as drug

carriers prepared from the In-g-PCL copolymer [6].

1.3. Inulin-Based Copolymers

Carla Sardo et al. synthesized the inulin-poly(lactic acid) (INU-PLA) copolymers to prepare doxorubicin-loaded nano-formulation for cancer treatment. They compared the PEG-PLA copolymer with the INU-PLA copolymer. It was found that the effectiveness of PEG, which is not a natural polymer, is reduced by anti-PEG antibodies. Due to the properties of inulin as a structural analog of the backbone, adhesion of cells, natural biocompatible polysaccharide that can be easily extracted from various plant sources, good solubility in water and organic solvents, non-toxicity, hydrophobicity, and flexibility, it was preferred for the synthesis of the copolymer [10].

The poly(acrylic acid) grafted inulin copolymer was synthesized by Mohammad M. Fares and friends. They aimed to increase the water solubility of the Irbesartan and to control the release rate of the drug with the poly(acrylic acid)-grafted inulin copolymer. The topological structure of inulin allowed the binding of the drug Irbesartan and its solubility with the increase of the amount of inulin in the copolymer [11].

Ugne Janciauskaite and Ricardas Makuska investigated a chitosan-inulin copolymer. Chitosan is limited in applications by insolubility at basic pH. The solubility of chitosan should be increased by modification with dextran and inulin, which have a linear chain structure, in water and organic solvents. Inulin was preferred due to its prebiotic activity and health-promoting potential, digestibility, lower caloric value, and water-binding capacity. While chitosan-N-dextran copolymers were soluble in water but their stability in aqueous solutions was low, chitosan-inulin copolymers were soluble in water over a wide pH range and formed viscous solutions; they were stable in aqueous solutions and had a high molecular weight [12].

1.4. Poly (ϵ -caprolactone)(PCL)

PCL is a linear, biodegradable, synthetic, and aliphatic polyester commonly used in pharmaceuticals [15, 16]. PCL has good processability and is easy to melt process. Thus, the copolymer can be easily synthesized [14]. Polycaprolactone, a biodegradable and biocompatible thermoplastic, has a longer shelf life than biopolymers that can

degrade in a short time, such as polylactic acid [15].

PCL can be prepared by two methods, such as polycondensation of 6-hydroxy caproic acid (6-hydroxy hexanoic acid) and ring-opening polymerization (ROP) of ϵ -caprolactone [21].

The condensation method can be performed by polycondensation of 6-hydroxy caproic acid under vacuum to remove water. Some enzymes can be used to increase the molecular weight of PCL [21].

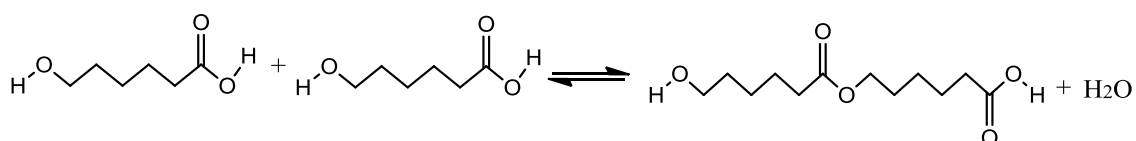


Figure 2. Polycondensation of 6-hydroxycaproic acid during PCL synthesis

The ROP process has been improved with various initiators, catalysts, and catalyst initiators.

Ring-opening polymerization (ROP) is a bulk process in which the cyclic ϵ -caprolactone monomers are mixed with a catalyst and the polymer is formed at high temperatures. Then, the polymerization product is cooled to room temperature and dissolved in an organic solvent and washed to remove the unreacted monomer and initiator [16]. The reaction for ROP can be seen in Figure 3.

Synthesis of PCL by ROP methods increases the molecular weight but decreases the polydispersity [21].

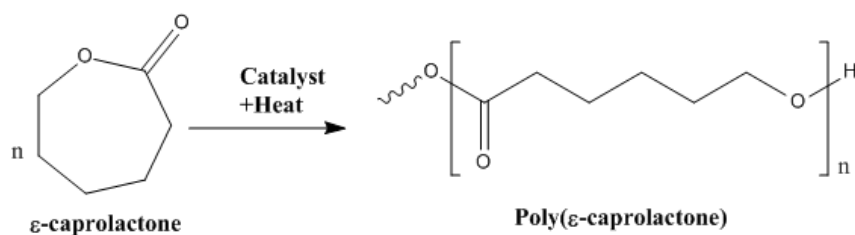


Figure 3. Ring-opening polymerization of ϵ -caprolactone [14]

1.4.1. Chemical structure and physicochemical properties

The chemical structures of caprolactone and PCL were presented in Figure 4.

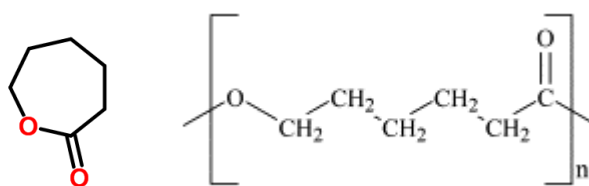


Figure 4. The structure of caprolactone and PCL

The molecular weight of PCL varies between 3,000 and 80,000 g/mole. Depending on the molecular weight, the melting point of PCL is between 59-64 °C [14]. The low melting point and low molecular weight facilitate the cell internalization of PCL and preparation of drug delivery systems by combining them with other polymers [16].

PCL is a semi-crystalline biodegradable polyester with a glass transition temperature (T_g) of -60 °C [14]. The degree of crystallinity of PCL reaches up to 69% [21]. The crystallinity of PCL decreases and crystallization temperature increases while the molecular weight increases [16].

The degradation of PCL starts from the end of the chain at higher temperatures, while it starts randomly in the chain at lower temperatures [21].

PCL is soluble in chloroform, dichloromethane, carbon tetrachloride, benzene, toluene, cyclohexane, and 2-nitropropane at room temperature. Nevertheless it has low solubility in acetone, 2- butanone, ethyl acetate, dimethylformamide, and acetonitrile. PCL is not soluble in alcohol, petroleum ether, and diethyl ether [14].

1.4.2. Applications of poly (ε-caprolactone)(PCL)

PCL and modified PCL are suitable for various applications due to the perfect properties such as low undesirable host reactions, biocompatibility, three-dimensional and directional porous structures [14].

PCL can be used to improve wound dressings, contraceptive devices, prostheses [14], and fixation devices [13].

PCL is suitable for long-term use due to its low biodegradability. Therefore, the choice of PCL offers an advantage in controlled drug delivery systems in biomedical fields. The fibers made from PCL can be used for implants, nerve guides, absorbable surgical sutures, and three-dimensional (3-D) scaffolds [14]. The properties of PCL adjust the

delivery of some hydrophobic drugs such as mesalazine, paclitaxel, curcumin, sulforaphane, and doxorubicin, so the use of PCL in drug delivery systems is desired [25].

1.5. Poly (ϵ -caprolactone)(PCL) Based Copolymers

PCL, which has great versatility, can be copolymerized by changing its mechanical, physical, and chemical properties. As a result, crystallinity, solubility, permeability, and degradation rate can be changed depending on the ratio of PCL in the copolymer for drug delivery [16].

The triblock copolymer PCL-PEG-PCL was synthesized by Hossein Danafar using the ROP method. Cancer and inflammatory diseases can be treated with curcumin, but there are some problems such as low bioavailability, short biological half-life, and low solubility due to low absorption. The synthesis of the PCL-PEG-PCL copolymer aimed to improve the bioavailability and water solubility of curcumin. Since curcumin is a hydrophobic drug, PCL was used as the hydrophobic core and PEG as the shell for the synthesis of the amphiphilic nanoparticles by the self-assembly method. PCL-PEG-PCL nanoparticles encasing curcumin developed the solubility of curcumin in water. The ratio of drug loading and encapsulation efficiency increased with increasing PCL. Moreover, they were a good vehicle for the controlled delivery of drugs in cancer therapy [17]. Similarly, Hakemii and friends also synthesized the triblock copolymer of PCL-PEG-PCL. They used the drug docetaxel to treat human liver cancer. However, the bioavailability, solubility, potentiation, and synergy of docetaxel were insufficient. PCL-PEG-PCL triblock copolymer as a nanocarrier was successfully used to improve the poor properties of docetaxel. Therefore, the PCL-PEG-PCL tri-block copolymer enhanced the effectiveness of docetaxel in inhibiting the cancer cells proliferation rather than normal cells [19].

In another study, Lio and friends synthesized the PCL–Pluronic–PCL copolymer using ROP method. The thermosensitivity and biodegradability of the copolymer were studied. The results showed that the phase transition temperature increased allowing the nanocarriers use in extended medical fields [20].

1.6. The Microwave Technology

Microwave technology has been used for the synthesis of PCL since 1986 [23]. Microwave radiation is absorbed selectively by bonds vibrating at the appropriate frequency, causing the molecule to heat up rapidly and rise to a higher energy level [18]. The dielectric loss during microwave absorption causes heating of the bulk. The electromagnetic waves transfer the energy to the molecule and results in some bonds to break and start the reaction [23]. Many polar molecules can be polymerized immediately due to the strong absorption by microwave energy [23].

There are some advantages of microwave technology; short reaction time, high reaction yield and conversion, low amount of by-product due to homogeneous distribution of radiation, easy scale-up [22]. Microwave method is simpler and less complicated compared to the traditional method [23]. Liquid crystal polymers, conductive polymers, optical materials and medical polymers are commonly synthesized by microwave irradiation [23]. In particular, the microwave method was preferred for the synthesis of PCL by ring-opening polymerization (ROP) of ϵ -caprolactone in the presence of acetic acid as an initiator, so metal catalyst was not necessary.

Xu and friends investigated the ring-opening polymerization (ROP) of ϵ -caprolactone on a large scale in microwave by varying the power between 850, 1700 and 2550 W with stannous octanoate ($\text{Sn}(\text{Oct})_2$) as catalyst. The variation of monomer mass and microwave power determined the reaction time and temperature. They obtained a high conversion of 94.1% by using 1500 grams of monomer at 850 W in about 96 degrees for about 40 minutes [33].

Liao and friends researched the ring opening polymerization (ROP) of ϵ -caprolactone using different microwave powers of 170, 340, 510 and 680 W. They used stannous octanoate ($\text{Sn}(\text{Oct})_2$) as the catalyst. The yield of PCL was higher at 680 W than at the other powers and was 90% for 30 minute [34].

Tan and friends investigated the ring-opening polymerization (ROP) of ϵ -caprolactone in microwave with hydrogen phosphonate. A 510 Watt microwave irradiation was used for 100 minute and hydrogen phosphonate served as a catalyst [35].

1.7. Coupling Reaction

The coupling reaction is a versatile and practical method using carbodiimide compounds for labeling or crosslinking with carboxylic acid [55]. The carbodiimides prevent the acid-base reaction and make the carboxylic acid susceptible to nucleophilic attack [56]. Carbodiimide compounds such as EDC (1-ethyl-3-(3-dimethylaminopropyl) carbodiimide) and DCC (dicyclohexylcarbodiimide) are used to activate carboxylic acids ($-\text{COOH}$) for conjugation with primary amines. While EDC is soluble in water by using an aqueous crosslinking, DCC is insoluble in water by using non-aqueous organic synthesis applications. The solvent of inulin and PCL is DMF, so DCC usage is appropriate in coupling reaction for the synthesis of PCL grafted inulin copolymer. The addition of NHS or Sulfo-NHS to coupling reactions increases efficiency [55].

Firstly, the imine deprotonates the carboxylic acid in Figure 5. The carboxylate group attack as a result forms an O-acylisourea intermediate. After an addition and elimination, product and side product as DCU obtain [56].

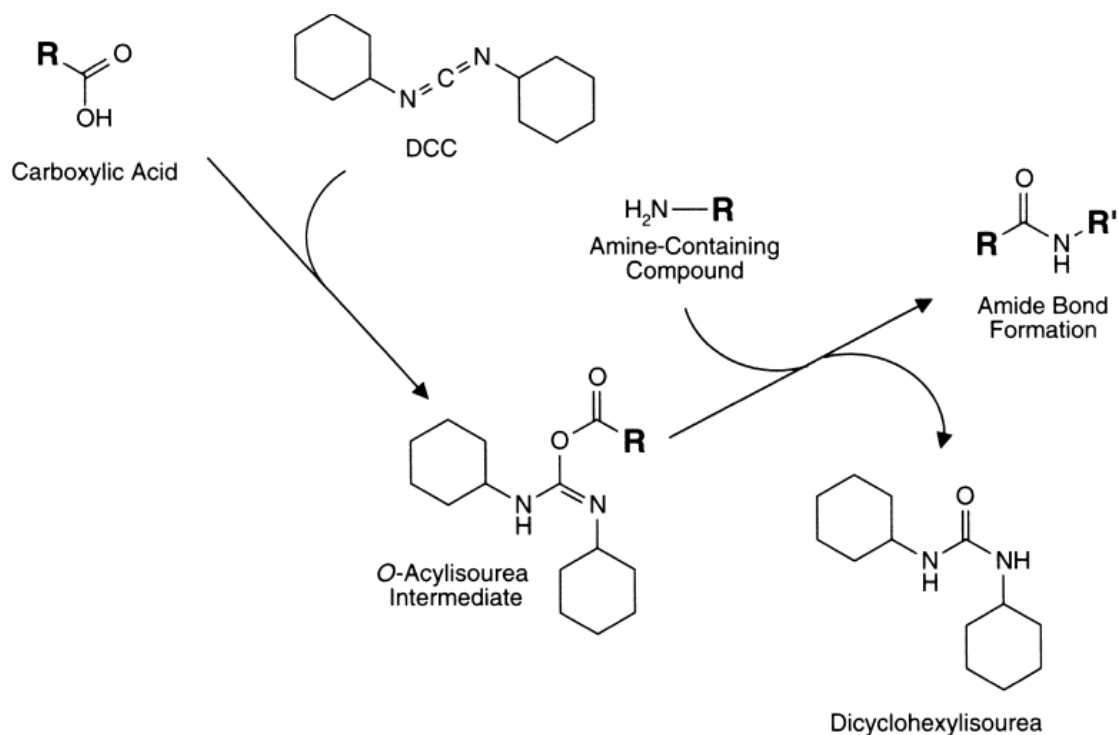


Figure 5. DCC coupling reaction mechanism [57]

1.8. Copolymers for Drug Delivery System

The number of cancer patients is increasing day by day in the world. Generally, cancer is treated with chemotherapy [28], but chemotherapy weakens the immune system by damaging both cancer cells and healthy cells. In addition, some of the drugs administered in the conventional way cause toxicity in the human body, and the concentration of these drugs is not necessary for the treatment of inflammatory bowel disease (IBD) for a long period of time. The goal is to treat the diseases by delivering the required drug only to the diseased cells, through targeted drug delivery. Therefore, amphiphilic and self-assembling nanodrug delivery methods offer the possibility of overcoming biological obstacles. These methods are non-toxic and allow controlled delivery. Thanks to amphiphilic structure, the nanoparticles can be immediately formed in physiological fluid.

In this thesis, inflammatory bowel disease (IBD) treatment was aimed with a targeted drug delivery system. Inflammatory bowel diseases (IBD) are a chronic and recurrent inflammations of the gastrointestinal tract. Chron's disease and ulcerative colitis essentially constitute this disease.

The drugs commonly used to treat IBS relieve the symptoms of inflammation, but over time cause an accumulation of toxicity and have severe systemic side effects. For this reason, research has developed nanoparticle-based drugs (NP) that are specifically used to treat the inflamed bowel [39].

1.8.1. Nanoparticle (NP)-based drug delivery system

NP-based drug delivery system improves the stability of the encapsulated drug, supplies controlled release to inflamed cells, and decreases the toxicity of the system. In addition, this system can reduce systemic bio-distribution and dosing frequency. There are several differences between the healthy and inflamed gut, such as pH, the colonic transit time, receptor expression, angiogenesis, and other microenvironmental factors. These differences offer advantages for targeted drug delivery in the inflamed gut based on NP. Smaller-sized NPs (<200 nm) were able to penetrate the mucus layer more deeply and reach intestinal tissue. NPs modified on the surface can remain in the target tissue for a while. In this way, intestinal imaging, therapeutic purposes and targeted

drug delivery can be realized [39].

Compared with similar drugs administered in conventional formulations such as tablets, capsules or emulsions, NP-loaded drugs offer higher efficacy at lower concentration. However, there are some problems, such as early release of the drug, poor targeting and toxicity of some synthetic nanomaterials used to produce the NPs [39].

The preparation of copolymers should overcome these problems. For this reason, inulin was selected because it has high targeting and stability, as it can be absorbed in both the small and large intestine. PCL was selected to hold the drug, intoxicity structure and supporting the physical properties of inulin. NP-based drug delivery system was formed by loading the drug into the PCL grafted inulin copolymer.

1.8.1.1. Self-assembly method

Self-assembly method is the spontaneous arrangement of individual units into highly ordered structures through interactions between the components themselves [29].

In nature, self-assembly forms in aqueous phases without the presence of organic solvents or surfactants. The organic solvents or surfactants have side effects for humans when used in drug delivery systems. Therefore, aqueous self-assembly of block copolymers is a harmless method for cancer treatment [30].

This method is the most versatile and simple strategy to improve nanostructures. Therefore, it is useful in many fields, such as physical, chemical, and biological sciences, material and biomedical sciences, and manufacturing [29].

Self-assembly of block copolymers with covalent nano-interactions can produce a variety of structures such as spherical micelles, vesicles, cylinders, and many others, depending on the medium [31]. The micelle has been seen to be useful among polymeric assemblies as the result of its functional or practical applications as a carrier for drug delivery [31].

The formation of micellar carriers requires an appropriate hydrophobic/hydrophilic balance with the conjugation of the hydrophilic polymer [25]. Micelles are formed as a result of this arrangement by balancing the attractive and repulsive forces [29].

The critical micelle concentration (CMC) is an essential parameter for micelle

formation [31].

Polymeric micelles form by self-assembly above the critical micelle concentration (CMC) with hydrophobic interactions [32]. An illustration of micelle formation can be seen in Figure 6.

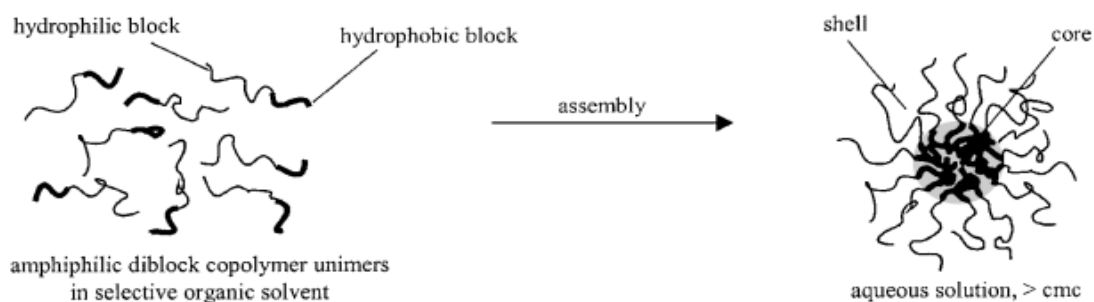


Figure 6. Micelle formation for an amphiphilic copolymer [27]

Numerous nano drugs in micelle structure have a hydrophobic part that supplies homogenous distribution of active substances as a core. Their hydrophilic part stabilizes an interface between the core and the outside aqueous medium as a shell [10].

There are many advantages of the micelles formed by amphiphilic copolymers as enhanced solubilization, drug efficacy, stabilization, and delivery of challenging agents [28]. The drug accumulation in diseased sites, permeability, and retention effects can be increased by decreasing the nanosize of polymeric micelle [28].

Therefore, the nanoparticles consisting of hydrophilic polysaccharide surface and hydrophobic inner core, are the promising future for targeting drug delivery. In the literature, drug delivery examples of inulin-based or PCL-based copolymers with self-assembly methods were detected.

As the first example, Mauro and friends synthesized the INU-EDAP and C-DOXO (inulin-pentyne and citraconic-doxorubicin) with self-assembly. This drug-loaded copolymer can reach the cancer sites and the maximum drug release rate was detected at pH imitating cancer tissue [26].

In the second example, Diao and friends synthesized the PEG-PCL copolymer by ring-opening polymerization of ϵ -caprolactone. The doxorubicin was encapsulated in the hydrophobic core by forming the structure of the micelles with self-assembly [28].

In this thesis, the hydrophobic part is PCL and the hydrophilic part is inulin. We fabricated the PCL grafted inulin copolymer (In-g-PCL) and loaded the nano/micro carrier with a hydrophobic model drug, mesalazine (mesalamine, 5-ASA, 5-Aminosalicylic acid). Both polymers are appropriate for the application of targeted drug delivery with non-toxic, biocompatible, and biodegradable properties. Thanks to inulin as a hydrophilic part, the drug can be transported in the body up to the large intestine without harm.

1.9. Mesalazine (mesalamine, 5-Aminosalicylic acid, 5-ASA)

Sulfasalazine which includes two parts sulfapyridine and 5-ASA was improved in the 1930s. The structure of 5-ASA was seen in Figure 7.

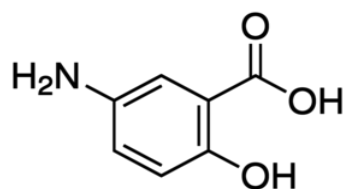


Figure 7. The chemical structure of 5-ASA [41]

5-ASA has many usages in research, while sulfapyridine has many side effects [40]. 5-ASA is an anti-inflammatory drug and it is used to treat inflammatory bowel disease (IBD) since the 1960s [41, 42]. The working mechanism of 5-ASA reduces the inflammation of the intestine and prevents the substance that causes the inflammatory [40]. In addition, the drug must be in direct contact with the intestine. The ways to take this drug are generally from the mouth or rectally [42].

5-ASA drugs are absorbed quickly [40], so the drug delivery system is important for the active ingredient to the inflamed site to reach the inflamed site.

While the common side effects of 5-ASA are seen as headache, nausea, abdominal pain, and fever, serious side effects of 5-ASA are seen as abdominal pain, rashes, pericarditis, liver problems, and kidney problems [42, 44]. The physicochemical properties of 5-ASA are listed in Table 2.

Table 2. The properties of 5-ASA [43,44]

Linear Formula, Formula	$\text{H}_2\text{NC}_6\text{H}_3\text{-2-(OH)CO}_2\text{H}$, $\text{C}_7\text{H}_7\text{NO}_3$
Synonyms	5-ASA, 5-Amino-2-hydroxybenzoic acid, Mesalamine, 5-Aminosalicylic acid
Molecular weight	153.14 g/mole
Color	Off-white to gray
Form	Powder
Storage temperature	2-8 °C
Solubility	1 M HCl:50 mg/mL, clear, yellow to brown
Melting point	283 °C

2. MATERIALS AND METHODS

2.1. Materials

ϵ -caprolactone, phosphate-buffered saline tablet (PBS) were purchased from Sigma-Aldrich. Inulin (Number average molecular weight, M_n is 3500 g/mole) was kindly supplied by Nante Kimya (TURKEY). Dimethylformamide (DMF), N, N'-Dicyclohexylcarbodiimide (DCC), N-hydroxysuccinimide (NHS), Acetic acid, and Tetrahydrofuran (THF) were supplied from Merck, Germany. 5-Aminosalicylic acid (Mesalamine, Mesalazine, 5-ASA) was purchased from Fluka Chemie AG (Switzerland).

2.2. Equipments

2.2.1. Microwave oven

Cem Mars 5 microwave accelerated reaction oven was used for the synthesis of PCL polymer.

2.2.2. Gel permeation chromatography-Light scattering (GPC-LS)

The number average molecular weight of the synthesized PCL was determined using a

Wyatt Dawn Heleos multi-angle light scattering instrument connected with a Wyatt Optilab differential refractive index detector (RI) (at 654 nm). A Perkin-Elmer 200 GPC high-pressure pump was used with a serial connected Styragel HR2, Styragel HR3, Styragel HR4E, and Styragel HR5E GPC column system. THF was used as a mobile phase at a 0.7 mL/min flow rate at 25 °C. PCL samples were dissolved in THF and filtered through a 0.45 µm filter before injection. The specific refractive index of PCL in THF was determined as 0.07 mL/g. The number average molecular weight of the synthesized PCL prepolymer was determined to be 1300 g/mole.

2.2.3. Fourier transform infrared spectroscopy (FT-IR)

The FT-IR spectra of PCL grafted inulin copolymer are recorded with Thermo Fisher Scientific Nicolet 6700 FT-IR spectrophotometer equipped with a Smart Orbit high-performance diamond attenuated total reflectance (ATR) accessories. Measurements were done in the range of 400-4000 cm⁻¹ in transmission mode.

2.2.4. Nuclear magnetic resonance spectroscopy (NMR)

The molecule structure of inulin, PCL, and PCL grafted inulin copolymer were determined by ¹H-NMR spectroscopy using Varian 600 MHz NMR at 25 °C. ¹H NMR spectra were recorded in CDCl₃+CF₃COOD mixture (for In-g-PCL) and in CDCl₃ (PCL-COOH).

2.2.5. Homogenizer

During the drug loading process, DAIHAN Scientific Homogenizer HG-15D homogenizer was used to emulsify the copolymer and drug.

2.2.6. Dynamic light scattering (DLS)

Particle size and size distribution of the particles and their zeta potentials were determined using a Nano-ZS Zen 3600 (Malvern, UK) model dynamic light scattering (DLS) instrument at 25 °C. Measurements were repeated three times for the drug loaded and unloaded samples and the results were averaged [43].

2.2.7. Lyophilizer

The nano/micro particle dispersion samples were freeze-dried at -60 °C and high vacuum using Christ model Alpha 2-3 LS Classic freeze dryer. After lyophilization their FTIR spectra and SEM images were recorded.

2.2.8. Scanning electron microscope (SEM)

Scanning electron microscopy (SEM) images of the drug-loaded and unloaded nano/micro samples were recorded using a HITACHI SU 5000 FEG-SEM-TEM&EDS instrument having a Schottky Gun and DEBEN-TEM detector. Well-dried creamy samples were applied on a conductive carbon sheet SEM images were recorded. SEM images were obtained at 25 kV, 5 kV, and 3 kV electron acceleration voltage and at different magnifications.

2.2.9. Shaking incubator

Drug release studies were performed using N-Biotek NB-205 model shaking incubator. The samples were shaken at 37 °C and at 150 rpm.

2.2.10. Ultraviolet-visible (UV-VIS) spectrophotometer

Agilent Technologies Cary 60 UV-VIS Spectrophotometer was used to follow the release of the drug from the nano/microparticles in PBS (pH 7.4). For measurements, 3 mL of the samples were taken at predetermined time intervals, and their absorbance was measured by UV-VIS spectrophotometer at 330 nm wavelength. The 5-ASA release profile and quantitative release analysis were performed using a previously prepared absorbance versus concentration calibration curve.

2.2.11. Differential scanning calorimetry (DSC)

Perkin Elmer Jade Differential scanning calorimetry (DSC) was used to determine the presence of the inulin and PCL segments of the In-g-PCL copolymer by determining their melting temperature and melting enthalpy. DSC data were evaluated by Pyris software. Measurements were performed at 10 °C/min heating rate under an argon atmosphere at 200 ml/min flow rate between 30 °C and 300 °C. Before measurements,

the DSC instrument was calibrated according to the indium melting point and enthalpy. For the baseline correction the measurement was run for an empty sample pan and baseline subtraction was performed.

2.2.12. Vacuum drying oven

The synthesized In-g-PCL copolymer samples were dried under vacuum at 30 °C using a MMM Medcenter Vacucell 22 Vacuum drying oven.

2.3. Methods

2.3.1. Microwave-assisted ring opening polymerization of ϵ -caprolactone

Microwave assisted ring opening polymerization (ROP) of ϵ -caprolactone (ϵ -CL) has generally been preferred for its rapidity, safety, high-temperature homogeneity, environmentally friendly, and efficiency properties. PCL was prepared with ring-opening polymerization (ROP) by using microwave oven. Some organometallic complexes have been reported in the literature as a catalyst in the ROP of ϵ -caprolactone [1, 2]. Considering that the use of a catalyst may cause undesired impurity and cytotoxicity problems and that low molecular weight PCL to be synthesized in this study will be used in drug carrier formulation, polymerization was carried out without using catalysis. Acetic acid was used as the initiator in the microwave-assisted ROP. For this, a mixture of 10 grams of ϵ -caprolactone monomer and 0.5 mL of acetic acid as initiator was prepared and added into a TEFLON tube. The tube was placed in the oven after the cap was tightly closed and the mixture was irradiated in a microwave oven (MW oven) to 600 Watts at 150 °C for 1 hour. The ROP mechanism is given in Figure 8.

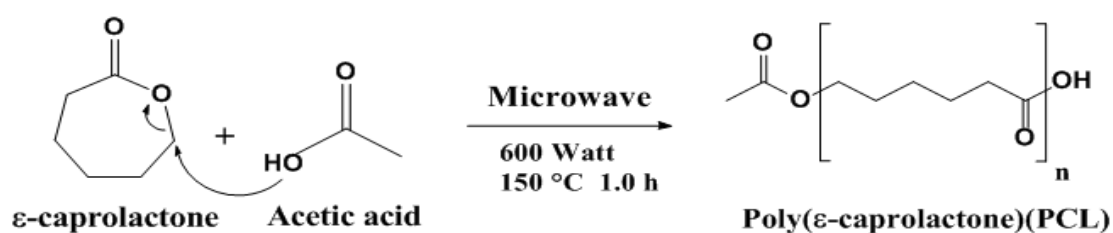


Figure 8. The synthesis of Polycaprolactone (PCL)

After irradiation, the tube was removed from the MW oven and cooled to room temperature. The polymerization mixture was dissolved in THF, and then the low molecular weight PCL was purified by precipitating it in water. The precipitated product was filtered, washed with water and methanol, and dried in a vacuum oven at 40°C yielding low molecular weight mono-carboxyl terminated PCL as a white solid (7.0 g, 70 %). The number average molecular weight (M_n) of the synthesized PCL prepolymer was 1300 g as determined by GPC-LS system.

2.3.2. Synthesis of PCL grafted inulin copolymer (In-g-PCL)

2-gram inulin was dissolved in 18 mL Dimethylformamide (DMF). To this solution a separately prepared solution of 1.0 gram of low molecular weight mono-carboxyl terminated PCL in 12 mL of DMF was added. This mixture was heated to 60 °C to obtain a homogeneous solution with stirring. To this clear solution, 0.52 g of N, N'-Dicyclohexylcarbodiimide (DCC) and 0.29-gram N-hydroxysuccinimide (NHS) were added. The reaction was continued at room temperature for 24 hours. After the esterification reaction was completed, the product was precipitated in water. Figure 9 shows the synthesis mechanism of the In-g-PCL copolymer.

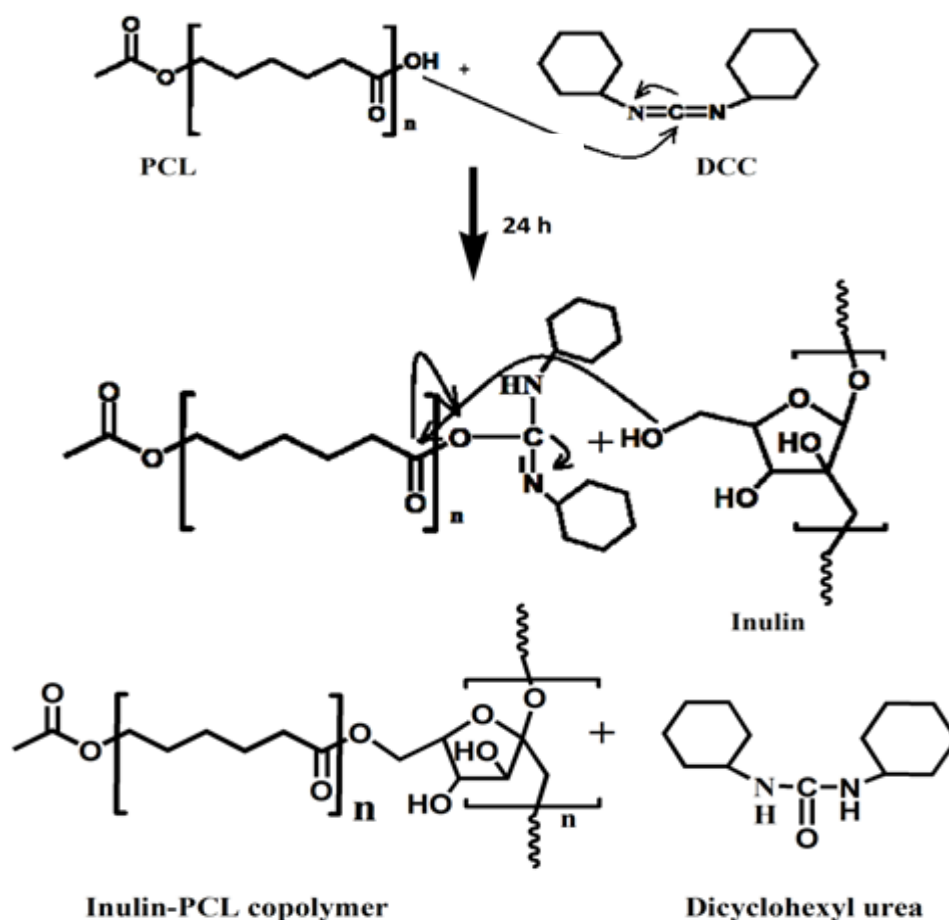


Figure 9. Synthesis mechanism of inulin-PCL copolymer

2.3.3. Drug loading process and release studies

2.3.3.1. Preparation of Nano/micro emulsion and Drug Loading

A solution of 4 mg of In-g-PCL copolymer in 5 mL of tetrahydrofuran (THF) was prepared in a 50 mL round bottom flask. To this solution, 1.0 mg of 5-ASA (Mesalazine, 5-aminosalicylic acid) was introduced. To get a more homogeneous and clear solution the RB flask was sonicated at 40 °C for 1.0 hour in an ultrasonic bath. After a clear solution was obtained, the flask was placed in the rotary evaporator, and the solvent was removed at 40°C under a vacuum. A thin polymer film was formed at the bottom of the RB flask. After further drying in a vacuum oven at 40 °C overnight 10 mL of PBS (pH 7.4) was added to the RB flask and subsequently mixed with a homogenizer at 1000 rpm. The amount of drug loaded on the prepared nano/micro dispersion was determined using UV-VIS spectroscopy.

2.3.3.2. Drug release studies

In order to obtain the release profile of 5-ASA from the nano/micro emulsion initially a calibration curve was obtained using 5-ASA solutions in PBS (pH 7.4) at different concentrations (0.005, 0.01, 0.015, 0.020, 0.025, 0.03, 0.035, 0.04, and 0.045 mg/mL). and a graph of absorbance versus concentration values of the samples was prepared using UV-VIS spectroscopy (Figure 10).

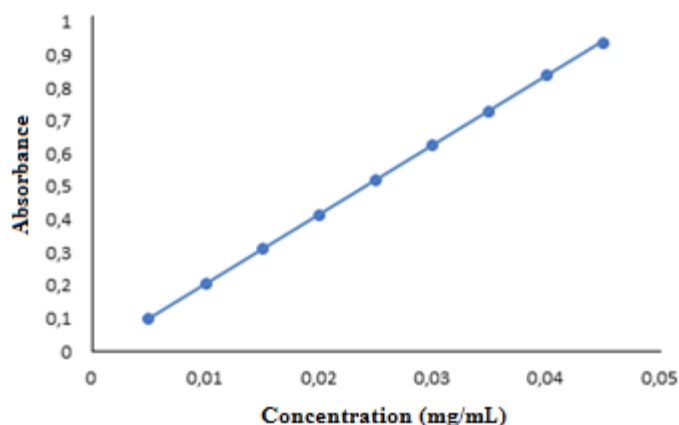


Figure 10. 5-ASA absorbance-concentration calibration curve

To follow the release of 5-ASA from the nano/microparticles, 5 mL of dispersion (1mg 5-ASA/10 mL* 5mL=0.5 mg of 5-ASA) was placed into a Slide-A-Lyzer MINI dialysis microtube (molecular weight cutoff of 3,500 Da, a product of Pierce, Rockford, IL) and dialyzed against 45 mL of PBS (pH 7.4). The dialysis tube was placed into the shaking incubator and shaken gently at 37°C and at 150 rpm for 145 hours. For each UV-VIS analysis, 3 mL of sample was taken from the PBS solution at different predetermined time intervals, and then their absorbance value at 335 nm was determined. Each sample was returned to the dialysis tube after the UV-VIS measurement. The analyzes were continued for 145 hours. The amount of the released 5-ASA was calculated by using the previously prepared calibration curve. The percentage released of 5-ASA versus the time graph is given in Figure 11.

According to calibration curve equation of 5-ASA in PBS;

$$\text{Absorbance}=21.02*(\text{Concentration at the time of measurement})-0.0042\dots\dots\dots(2.1)$$

$$R^2=0.9999\dots\dots\dots(2.2)$$

The released amount of 5-ASA calculation;

$$\frac{(\text{Absorbance value} + 0.0042)}{21.02} \text{mg/mL} * V(43 \text{ mL}) \dots \dots \dots (2.3)$$

The percentage released of 5-ASA calculation;

$$\frac{\text{The released amount of 5-ASA}}{Mi(0.5\text{mL})} * 100 \dots \dots \dots (2.4)$$

V is the value the volume of the PBS solution in the tube (45 mL) and Mi is the value the initial weight of drug within the micelles.

The final volume of the solution in the tube is measured as 43 mL.

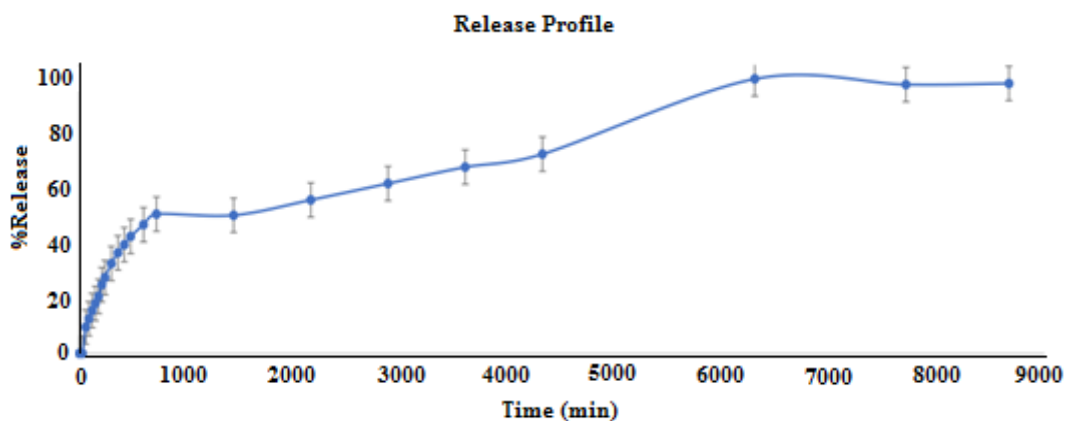


Figure 11. % Released of 5-ASA versus time graph

The amount of drug remaining in the micelles present in the dialysis micro tubing was determined by bursting them in PBS:dimethylformamide (DMF) (1.5:2) followed by analyzing them with a UV-VIS spectrophotometer. Figure 12 shows the calibration curve of absorbance versus concentration of 5-ASA in DMF.

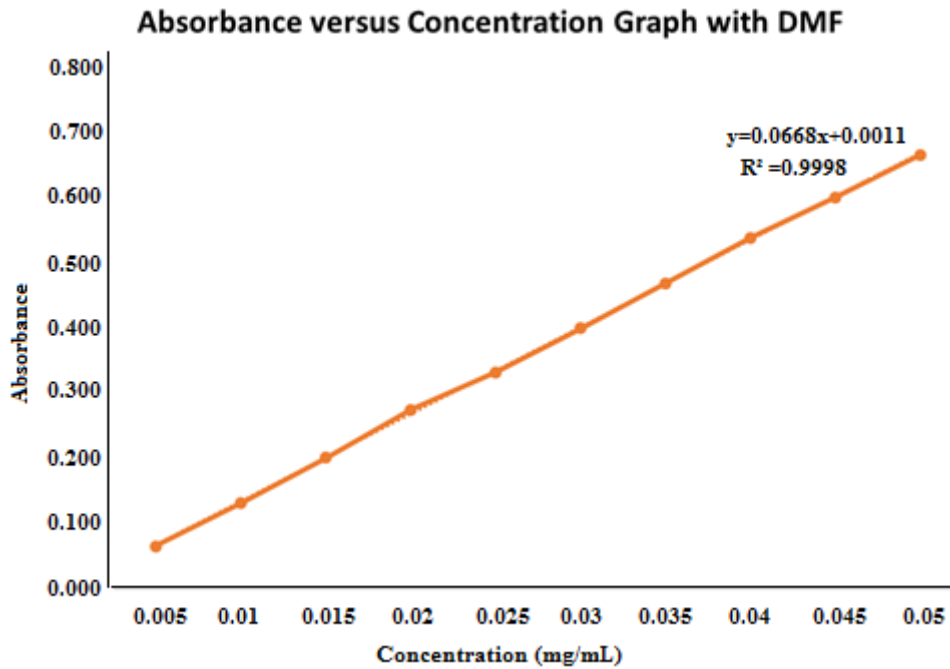


Figure 12. 5-ASA absorbance-concentration calibration curve in 1.5:2 PBS:DMF

According to Figure 12, the calibration curve equation of 5-ASA in 1.5:2 PBS: DMF has been used for the calculation.

$$\text{Absorbance} = 0.0668 * (\text{Concentration}) + 0.0011; R^2 = 0.9998 \dots (2.5)$$

$$m = C * v \dots (2.6)$$

$$\text{Remaining drug \%} = m/m_i * 100 \dots (2.7)$$

C is the calculated concentration of the remaining drug, v is the volume of micelle solution (5mL – initial volume, or 3.72 mL volume after the drug release), m is the weight of the measured drug, and m_i is the initial weight of drug within the micelles.

No absorption has been detected at 335 nm wavelength, at which 5-ASA is normally detected within 1.5:2 PBS: DMF solution.

Since the last drug release measurement from the tube suggested that the micelle has released the drug 100%, it can be concluded that the absorbance at 325-330 nm is not from the drug and no drug has been detected.

3. RESULTS AND DISCUSSION

3.1. Spectroscopic Characterization

The reaction between inulin and PCL was evaluated by recording the FT-IR and ^1H -NMR spectra of inulin, PCL, and In-g-PCL copolymer.

3.1.1. FTIR Analysis

Figure 13 shows the FT-IR spectrum of PCL. The characteristic strong absorption peak at 1718 cm^{-1} are assigned to the $\text{C}=\text{O}$ vibrational stretching of the ester groups [46]. The peaks at 2863 and 2943 cm^{-1} are due to the two different $\text{C}-\text{H}$ stretching absorption of PCL. The peak at 1163 cm^{-1} is due to the bending absorption of $\text{CO}-\text{O}-\text{C}$ groups of PCL. The deformational bending vibration of the two different $\text{C}-\text{H}$ bonds are observed as weak absorption bands at 1470 cm^{-1} , 1362 cm^{-1} , and 730 cm^{-1} .

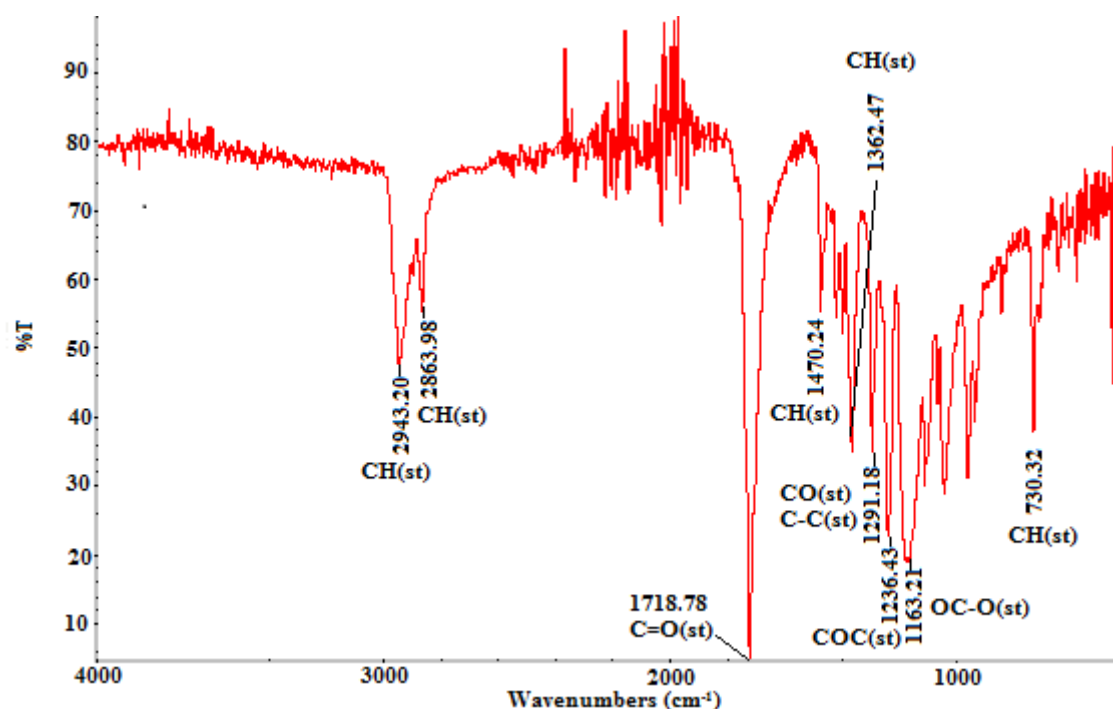


Figure 13. FTIR spectrum of PCL

Characteristic IR absorption peaks of inulin are also reported in the literature [47]. As shown in Figure 14, a broad absorption band between $3200\text{--}3500\text{ cm}^{-1}$ is due to the $-\text{OH}$ groups of inulin fructose units. The peaks observed at 2928 cm^{-1} and 2910 cm^{-1} were assigned to the $\text{C}-\text{H}$ stretching absorption of the fructose rings. The weak intensity peak

observed at 1428 cm^{-1} is due to C-H bending vibration of the fructose rings of inulin. The major absorption peaks that appeared at 1026 cm^{-1} and 986 cm^{-1} are due to the C-O-C symmetric bending vibrational absorption of inulin.

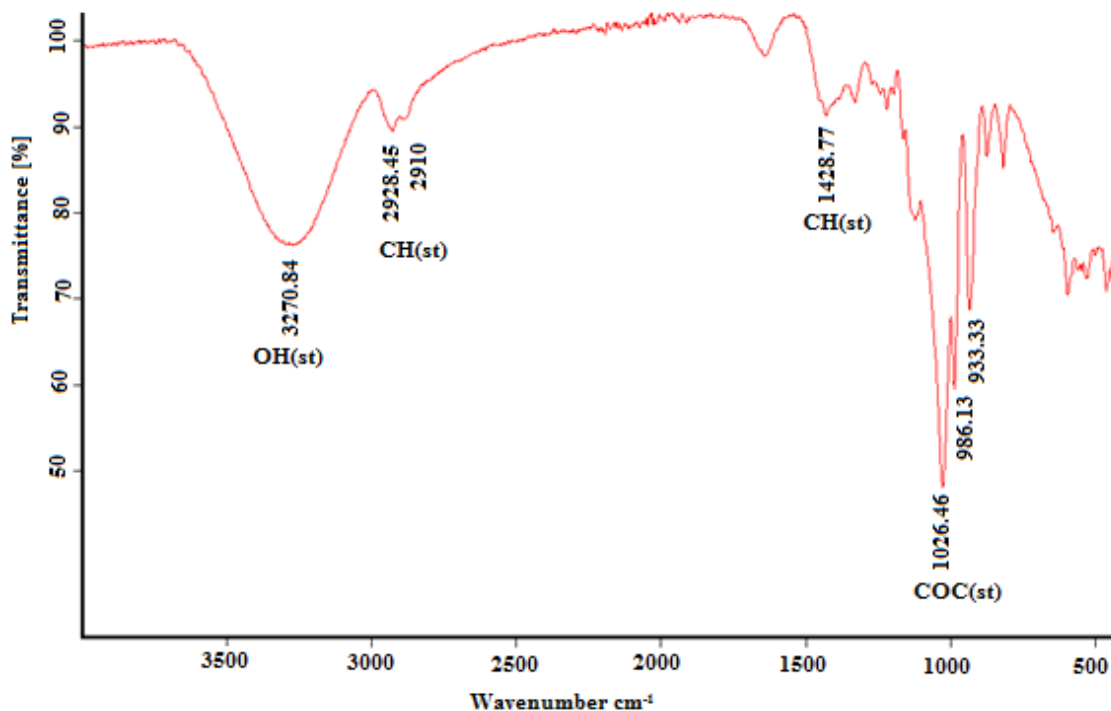


Figure 14. FT-IR spectrum of inulin

The FT-IR spectrum of In-g-PCL copolymer is shown in Figure 15. The characteristic absorption peaks of PCL; C=O ester stretching absorption at 1720 cm^{-1} , C-H stretching absorption at 2864 cm^{-1} and 2929 cm^{-1} , and the weak C-H bending absorption peaks at 1435 cm^{-1} and 1396 cm^{-1} are observed. In addition to these PCL peaks, the peak at 3317 cm^{-1} was assigned to the -OH stretching absorption of the fructose rings and the strong absorption bands at 1174 cm^{-1} and 1237 cm^{-1} are due to the C-O-C symmetric bending vibration of inulin [45]. Since the C-H stretching absorption peaks of inulin overlapped with that of PCL's peaks, they did not appear as separate peaks in the spectrum. The characteristic IR absorption peaks of PCL and inulin evidenced the In-g-PCL copolymer's successful synthesis. This was supported by ^1H NMR spectroscopy as well.

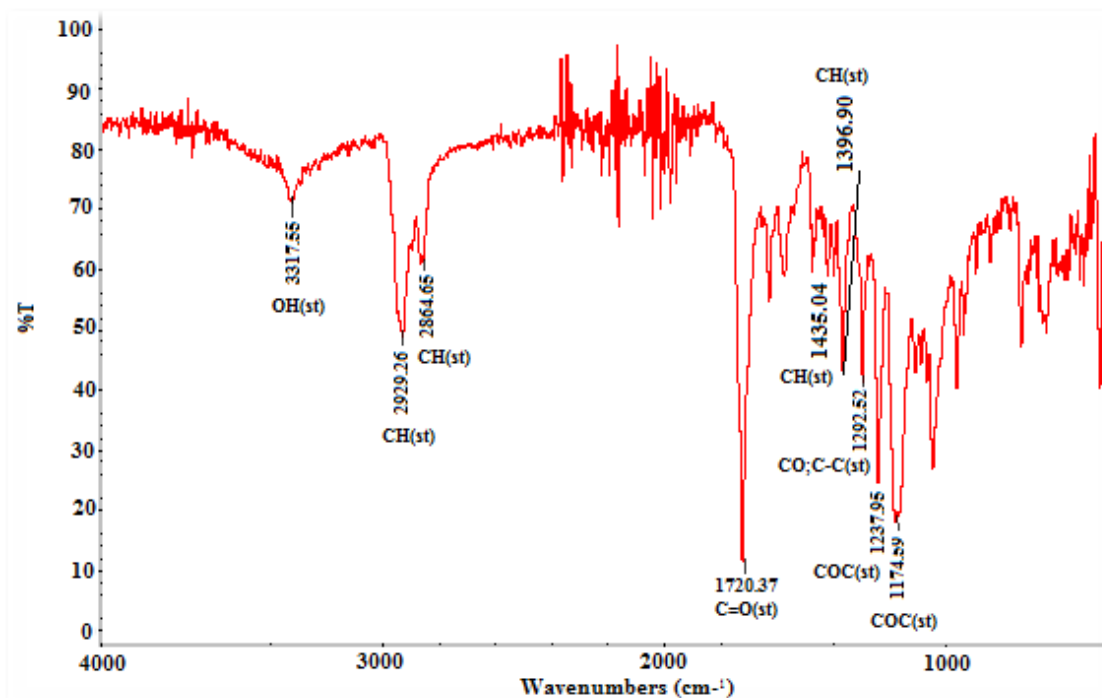


Figure 15. FTIR spectrum of In-g-PCL

3.1.2. NMR Analysis

^1H NMR spectroscopy was used for the detailed investigation of the chemical structure of In-g-PCL copolymer. For this purpose, the ^1H NMR spectra of inulin, PCL, and the synthesized In-g-PCL copolymer were recorded. ^1H NMR spectrum of PCL is shown in Figure 16. Proton peaks of PCL at (ppm) H1(1.37), H2(1.63), H3(2.3), H4(4.05), CH_2 protons of terminal $-\text{CH}_2-\text{COOH}$ group (2.36) and carboxylic acid proton (COOH) (2.04) are observed. The carboxyl termination of the PCL prepolymer synthesized by the acetic acid initiated microwave polymerization was demonstrated by the appearance of proton peaks of the $-\text{CH}_2-\text{COOH}$ and COOH groups at 2.36 ppm and 2.04 ppm, respectively.

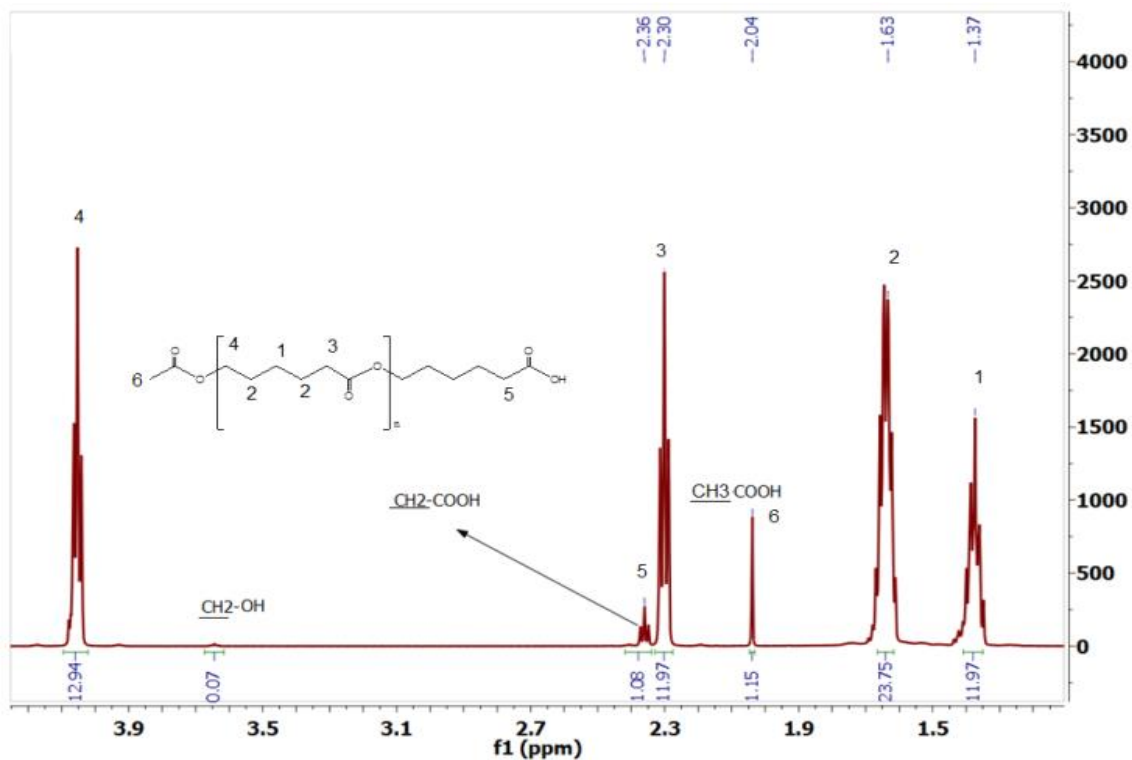


Figure 16. ¹H NMR spectrum of PCL

In the ¹H NMR spectrum of inulin (Figure 17) the characteristic proton peaks of the fructose ring at (ppm) H1(3.57, 3.73), H3(4.12), H4(3.97), H5(3.79) and H6(3.73, 3.64) are observed.

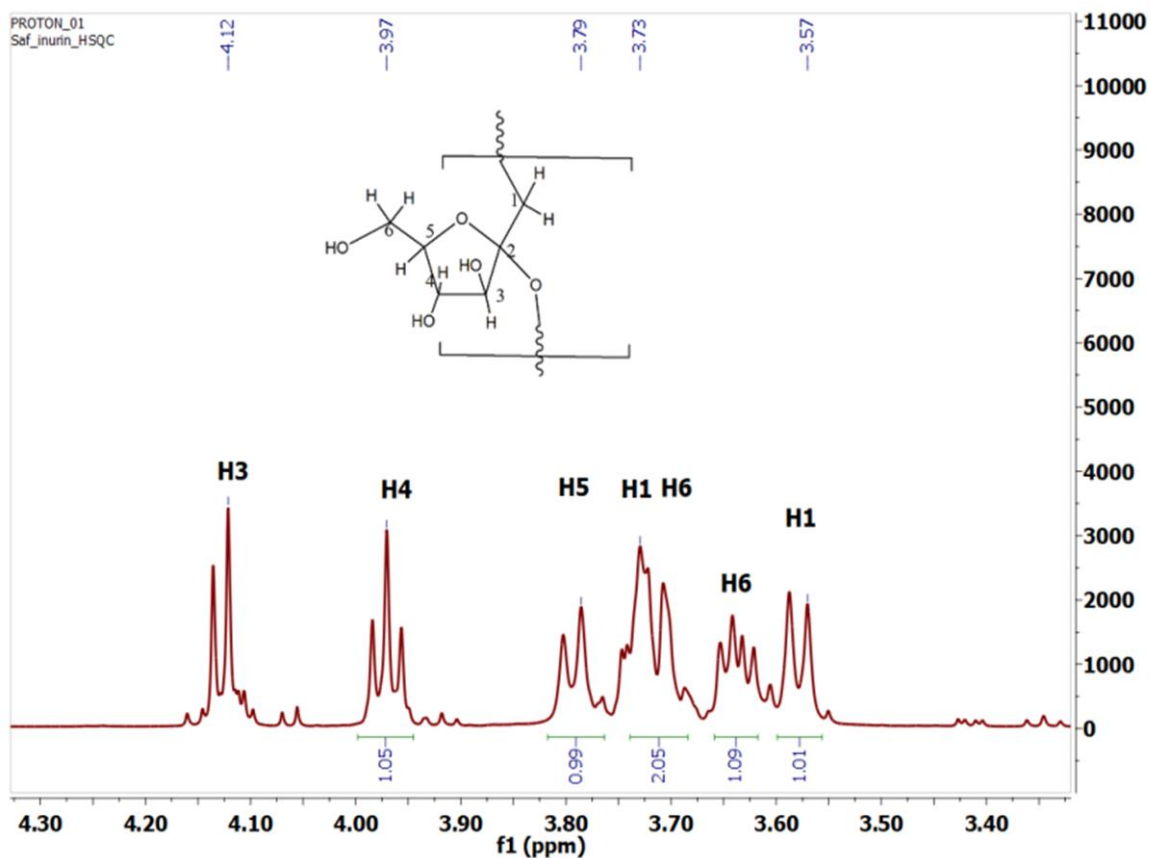


Figure 17. ¹H-NMR spectrum of inulin

In-g-PCL copolymer was synthesized through the carbodiimide coupling reaction of the carboxylic acid (COOH) end groups of PCL and hydroxymethyl (CH₂-OH) groups of inulin. It was difficult to find a suitable solvent system for the NMR spectrum of the copolymer, since inulin and PCL have quite different polarity. Although we have tried many amphiphilic solvents, we could not determine a good solvent for the NMR measurements. Therefore, we obtained the best result for the CDCl₃+CF₃COOD mixture in ¹H NMR studies. Proton chemical shifts (δ) of inulin are clearly observed between 3.7 ppm and 4.4 ppm (Figure 18). Due to the solvent effect, PCL peaks made some shifts.

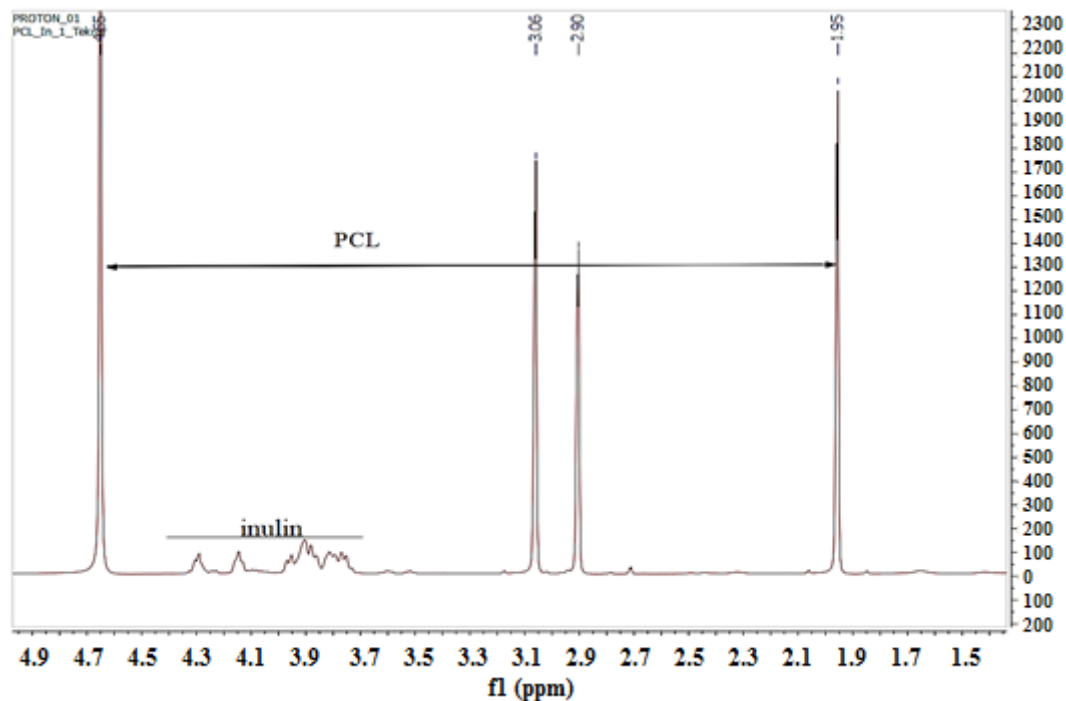


Figure 18. ^1H -NMR spectrum of copolymer (In-g-PCL)

3.2. Differential Scanning Calorimetry (DSC) Analysis

The melting behavior of the In-g-PCL copolymer was determined using a Perkin-Elmer Pyris DSC instrument with an auto cooling system and Pyris software. It was known that the melting point of pure inulin is in the range of 165 to 188 °C [51], while the melting point of pure PCL is 60 °C [52] and the glass temperature of pure PCL is approximately -60 °C [52]. For the DSC analysis 10 mg of the copolymer was heated from 10°C to 280°C to determine the melting points of the copolymer components. Since being in the out of heating range, the glass transition temperatures of the copolymer components were not determined in this study. As shown in Figure 19 the DSC thermogram of the copolymer sample has two endothermic peaks at 54 °C and 182 °C. The first endotherm is due to the PCL melting with a melting enthalpy of $\Delta H=81$ J/g and the second endotherm is due to the melting of inulin with a melting enthalpy of $\Delta H=8.36$ J/g. As reported in the literature, the melting point of PCL and inulin depend to some extent on the molecular weight [51, 52]. The presence of two melting temperature on the DSC thermogram is additional proof of the copolymer synthesis.

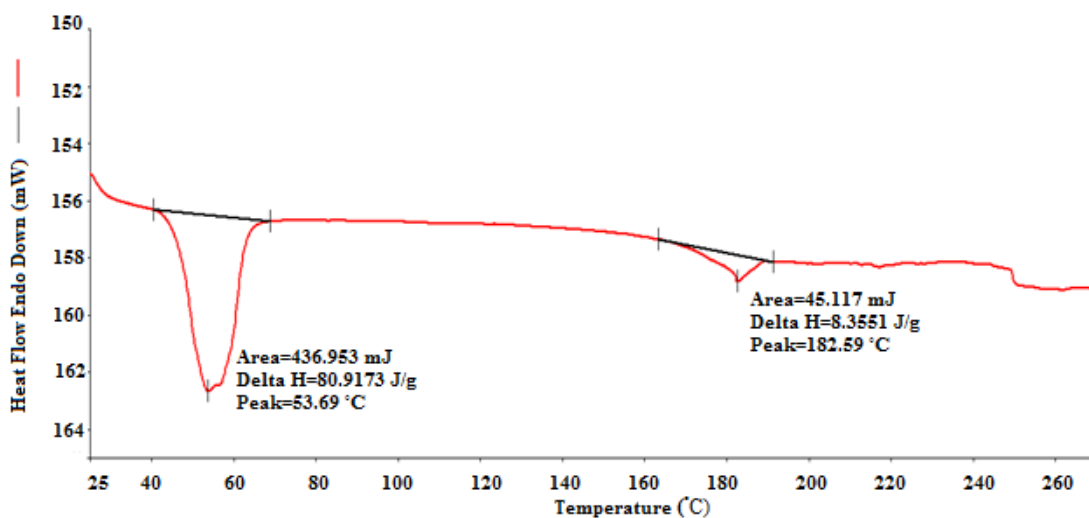


Figure 19. DSC thermogram of In-g-PCL

3.3. SEM Analysis

Scanning electron microscopy (SEM) is a useful technique for determining the morphological structure of materials. Therefore, the shape, size, and size distribution of the particles prepared by emulsification of In-g-PCL copolymer in PBS (pH 7.4) were visually observed before and after 5-ASA loading. After emulsification, the particles were isolated by centrifugation and obtained in creamy form. The test samples were applied on a conductive carbon strip and their SEM images were obtained. Figure 20 shows the SEM image of the nanoparticles before 5-ASA loading. After emulsification, the copolymer turned into a stable micelle structure at the nanometer scale. They are spherical in shape and have a nearly smooth surface, and uniform size and size distribution. As observed from this figure the particles are partly embedded in the linear copolymer matrix.

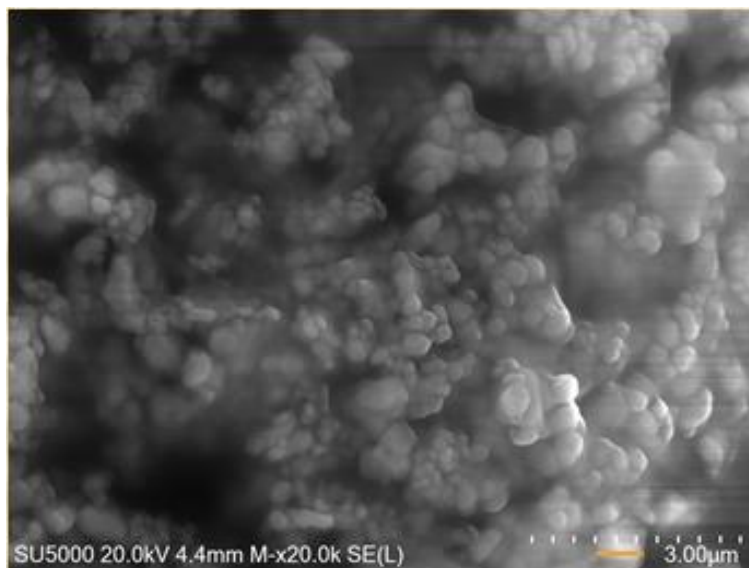


Figure 20. SEM image of the In-g-PCL particles before 5-ASA loading

Figure 21 shows the SEM images of the 5-ASA loaded micelles at different magnifications. The size of the micelles increased after 5-ASA loading and more deformed surface was observed.

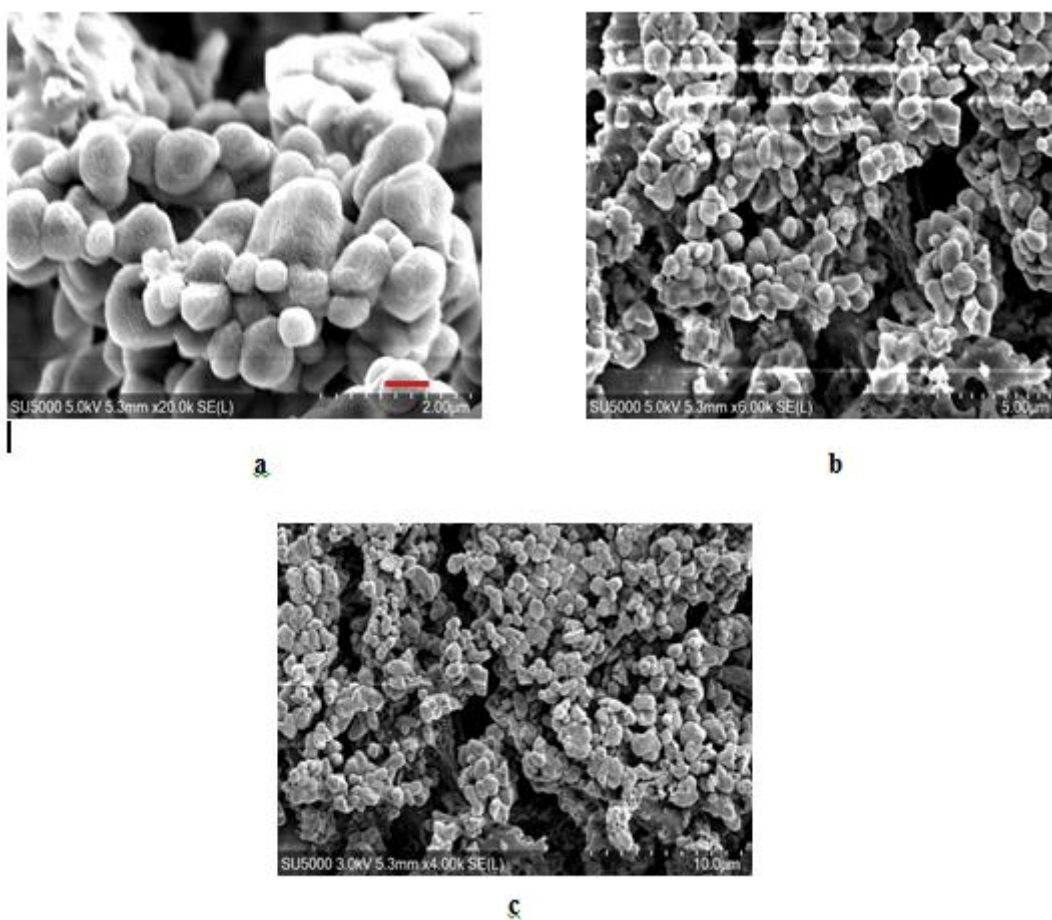


Figure 21. SEM images of the 5-ASA loaded In-g-PCL copolymer particles at a)20.000 b)6.000 c)4.000 magnifications.

3.4. Particle Size Distribution and Zeta Potential

Particle size, size distribution, and zeta potential of the In-g-PCL dispersion were measured using a dynamic light scattering (DLS, Malvern, UK model) instrument. As shown in Figure 22, the 5-ASA unloaded micelles were average 600 nm in size with a relatively narrow particle size distribution and the zeta potential was determined as -4.49 mV, which can be taken as evidence of the stable micelle formation.

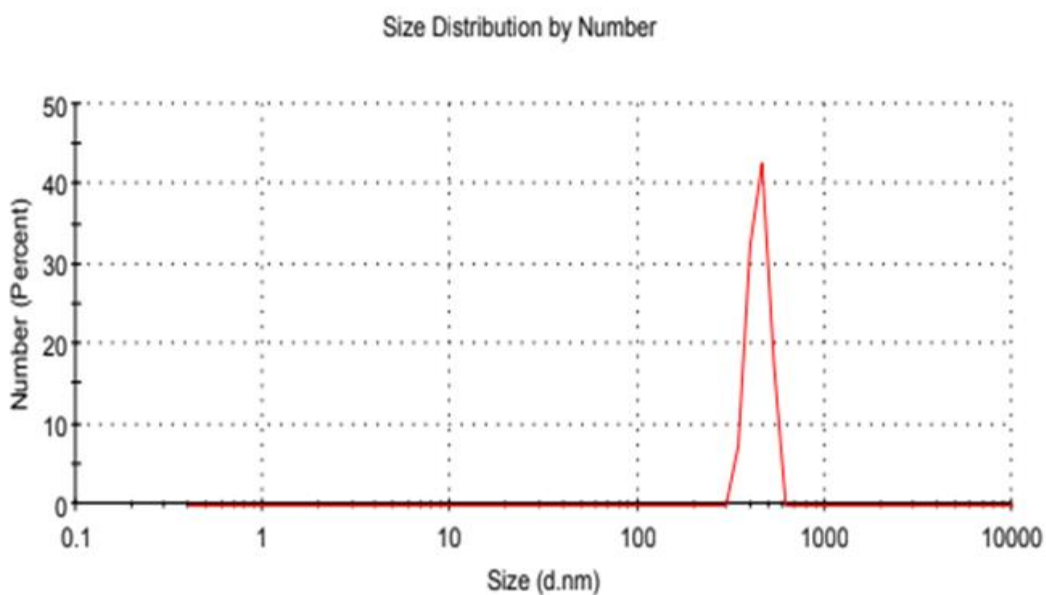


Figure 22. Particle size distribution of the 5-ASA unloaded In-g-PCL micelles.

Figure 23 shows the particle size and size distribution of the 5-ASA loaded In-g-PCL dispersion. The average particle size of the 5-ASA-loaded micelles was measured to be 883 nm and the zeta potential was -6.65 mV. The average particle size of the micelles increased after 5-ASA loading. The wider particle size distribution compared to the unloaded samples was observed.

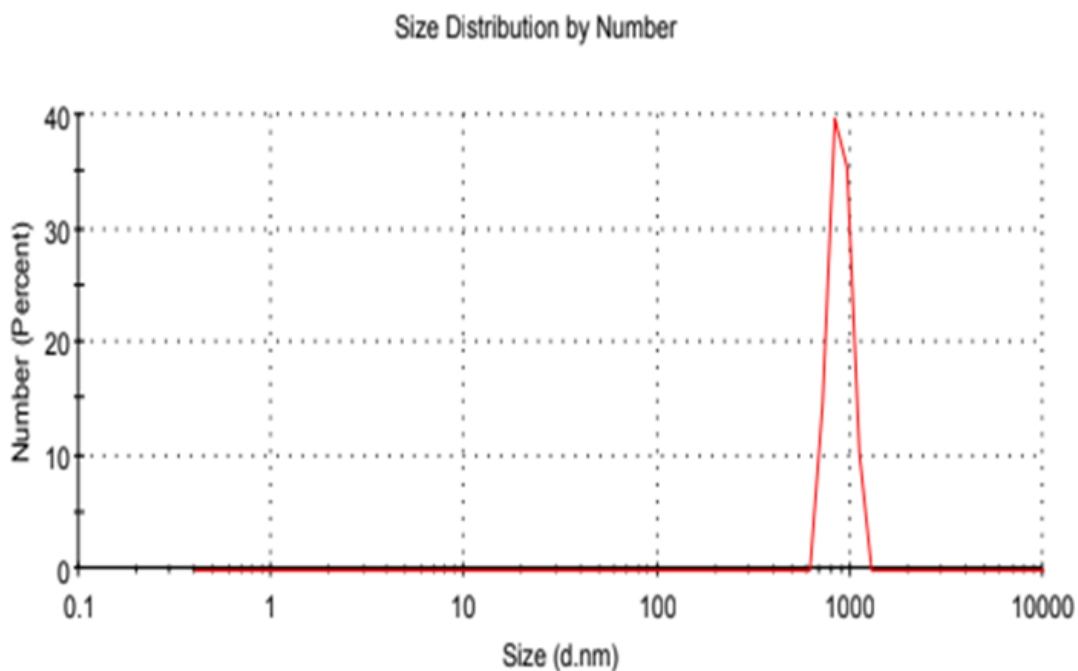


Figure 23. Particle size distribution of the 5-ASA loaded In-g-PCL micelles.

The thickness of the mucus layer in the intestine is 700 μm . Barua et. al., (2013) determined the pore size of tumor vasculatures in the range from 380 to 780 nm [48]. Therefore, drug-loaded PCL-grafted inulin particles were considered to be suitable for tumor treatment in the large intestine. The Zeta potential of the nanoparticles demonstrates the electrostatic potential at the electrical double layer covering a nanoparticle in solution, which affects the drug release stability, release rate, and absorption in the cellular membranes [50]. Most of the cellular membranes are negatively charged [49].

Since the zeta potentials of PCL grafted inulin nanoparticles with drug and without drug were within the range of -10 and $+10$ mV which is accepted as neutral [49], they were concluded to be suitable for penetration to the cellular membrane. The zeta potentials of PCL grafted inulin nanoparticles with drug and without drugs were neutral, so they were suitable for penetration into the cellular membrane.

3.5. Drug Release Studies

Release analysis of 5-ASA from PCL grafted inulin particles was performed using UV-VIS spectroscopy at $37\text{ }^{\circ}\text{C}$ and 330 nm. The amount of 5-ASA release was determined by converting the measured absorbance values to concentration using a previously prepared absorbance-concentration calibration curve.

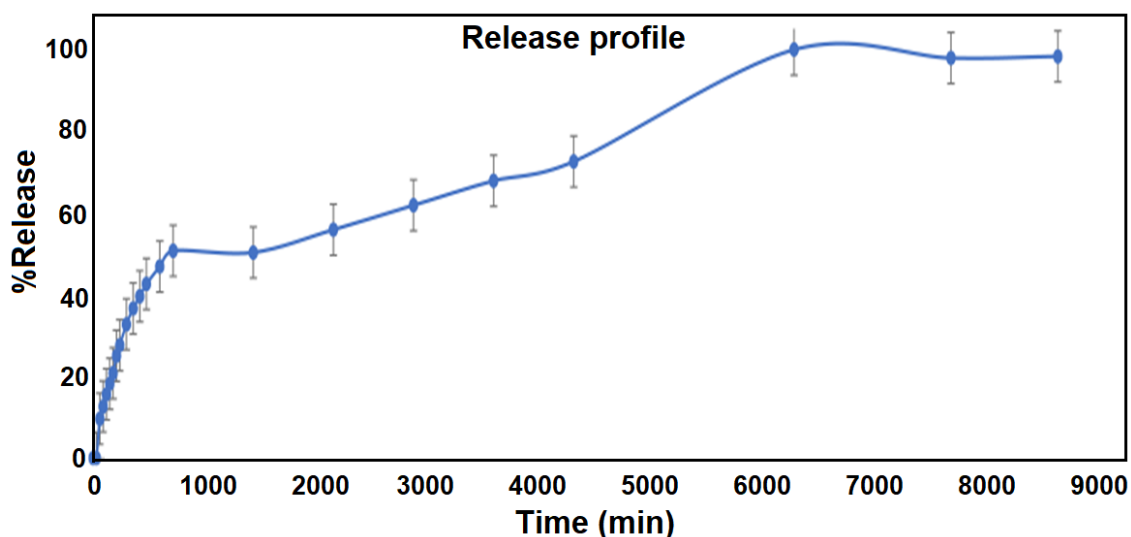


Figure 24. Release profile of 5-ASA from the In-g-PCL micelles.

It was observed from Figure 24 that 96% of 5-ASA was released at 144 hours. The kinetic analysis of the controlled drug release is very important to understand the factors affecting release behavior, release rate, and efficacy [53]. Thus, different kinetic models were studied to determine the best drug release profile. The correlation coefficients (R^2) of kinetic models were calculated as 0.8219 in the zero order, 0.716 in the first order, 0.0239 in Korsmeyer Peppas, and 0.8916 in Hixon-Crowell. The highest R^2 value was determined as 0.8916 in Hixon-Crowell when compared to other kinetic models. Therefore, the Hixon-Crowell method shown in Figure 28 was found suitable for the 5-ASA release from PCL grafted inulin copolymer.

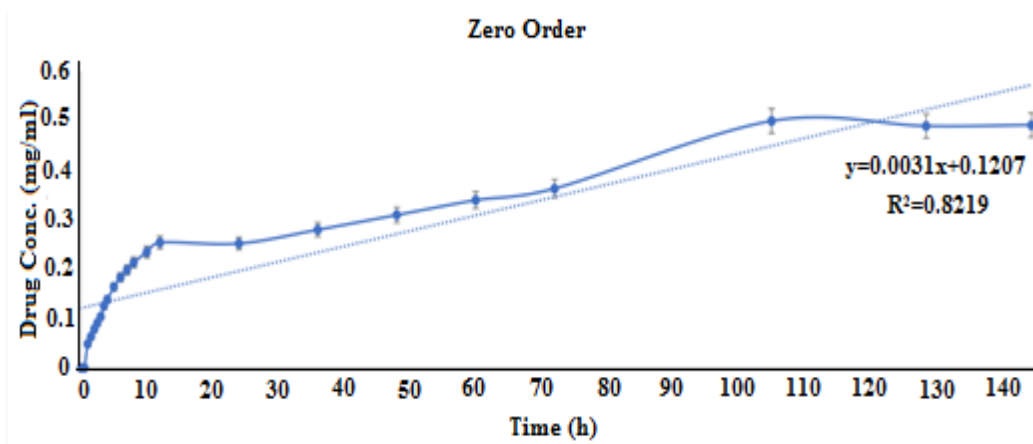


Figure 25. Zero Order Model

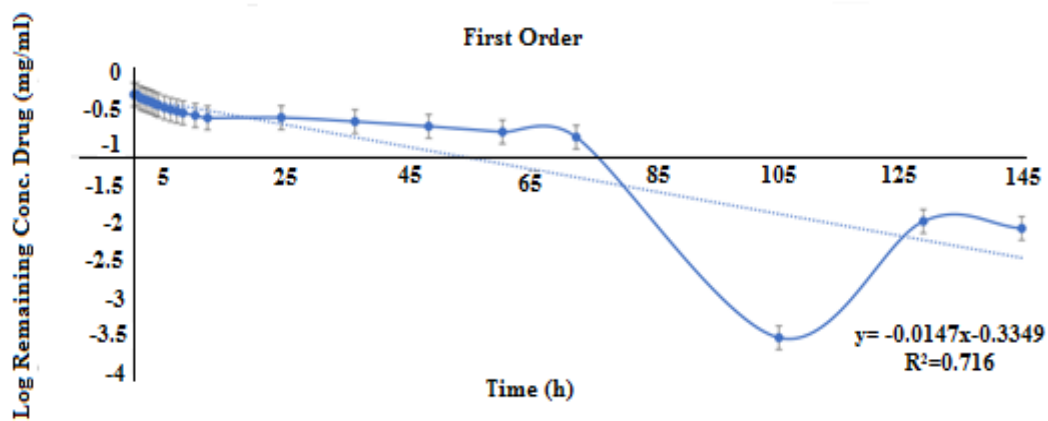


Figure 26. First Order Model

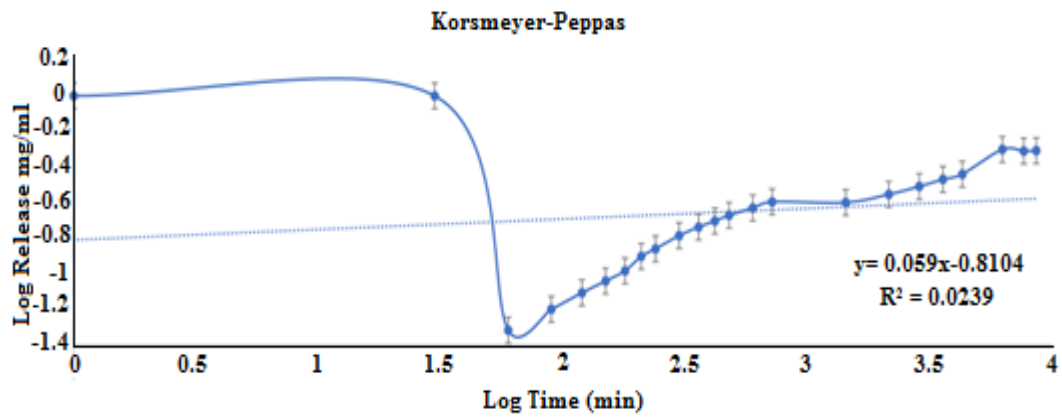


Figure 27. Korsmeyer-Peppas Model

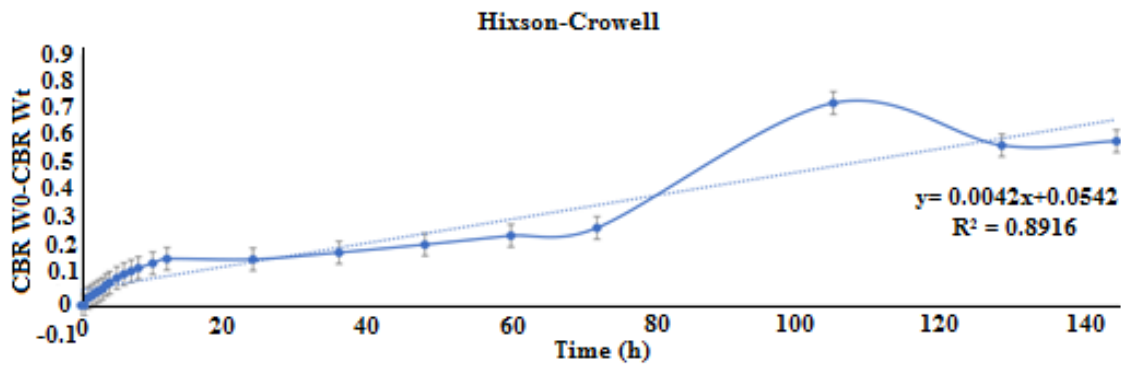


Figure 28. Hixson-Crowell Model

Since the release profile was identified as fitting the Hixson and Crowell cube root law the drug release was concluded to depend on the surface area and diameter of particles [54]. This means the release rate in this model can be controlled by the drug particle's dissolution rate, not diffusion [54].

4. CONCLUSION

In this thesis, carboxyl-terminated low molecular weight PCL was synthesized by microwave-assisted ROP and grafted onto inulin by a DCC coupling reaction via its -CH₂-OH groups. The synthesized In-g-PCL copolymer was emulsified in PBS and nano/micro micellar particles were obtained. Before 5-ASA loading, while the average particle size of the micelles was 600 nm, which increased to 883 nm after 5-ASA loading.

The chemical structure of inulin, PCL, and PCL grafted inulin copolymer (In-g-PCL) was investigated using FTIR and ¹H NMR techniques. The presence of the characteristic peaks of PCL and inulin were observed in the FTIR and ¹H NMR spectra. The proton peaks of the -CH₂-COOH groups in the ¹H NMR spectrum of PCL evidenced the PCL polymerization was terminated with COOH groups. In the ¹H NMR spectrum of the copolymer the characteristic peaks of inulin and PCL were observed, which confirmed the successful copolymer synthesis. In the DSC analysis of copolymer the melting points of inulin and PCL were clearly observed at 182 °C and PCL at 54 °C, respectively.

The morphological structure and particle size analyses of the prepared nano/micro micelles were performed by SEM and DLS techniques before and after 5-ASA loading. An increase in micelle size and surface defects were observed after 5-ASA loading. The spherical and stable micelles with a uniform size distribution (600 nm average particle size) were observed before 5-ASA loading, while the average particle size was 883 nm after drug loading. It is notable that their negative zeta potential values were suitable for penetration of the micelles into the cellular membrane.

Drug release studies were performed using UV-VIS spectroscopy in PBS (pH 7.4). The release profile was achieved using the previously prepared absorbance-concentration curve, and it was observed that 96% of 5-ASA was released at 144 h. Kinetic models were calculated to determine drug release behavior. When different models were compared, the Hixson-Crowell Model had the highest correlation coefficient (R^2) of 0.8916. Thus, it was determined that drug release behavior could be controlled with the size and surface area of particles.

REFERENCES

1. Boeckner, L.S., Schnepf, M.I., Tunland, B.C., (2001). *Inulin: A Review of Nutritional and Health Implications*. Advances in Food and Nutrition Research Vol. 1-63.
2. Ahmed, W., Rashid, S., (2019). *Functional and therapeutic potential of inulin: A comprehensive review*. Critical reviews in food science and nutrition, 59(1), 1-13.
3. Franck, A., (2002). *Technological functionality of inulin and oligofructose*. British Journal of Nutrition, 87(S2), 287-291.
4. Kesharwani, P., Paknikar, K. M., Gajbhiye, V., (2019). *Polymeric Nanoparticles as a Promising Tool for Anti-cancer Therapeutics*. Academic Press, 293-318.
5. Hilman, A., Harmayani, E., Cahyanto, M. N., (2018). *Inulin Extraction and Characterisation of Fresh and Chip Gembili (Dioscorea Esculenta) Extract by Ultrasound-assisted Extraction*. Proceedings of the International Conference of Science, Technology, Engineering, Environmental and Ramification Researches (ICOSTEERR), Vol. 1, 47-53.
6. Afinjuomo, F., Abdella, S., Youssef S.H., Song, Y. and Garg, S., (2021). *Inulin and Its Application in Drug Delivery*. Pharmaceuticals, 14(9), 855.
7. Mudgil, D., (2017). *The interaction between insoluble and soluble fiber*. In Dietary fiber for the prevention of cardiovascular disease, Academic Press, 35-59.
8. Niness, K.R. (1999). *Nutritional and Health Benefits of Inulin and Oligofructose*.
9. Stevens, C.V., Meriggi, A. and Booten, K., (2001). *Chemical Modification of Inulin, a Valuable Renewable Resource, and Its Industrial Applications*. Biomacromolecules, 2(1), 1-16.
10. Sardo, C., Mencherini, T., Tommasino, C., Esposito, T., Russo, P., Gaudio, P.D. and Aquino, R.P., (2021). *Inulin-g-poly-D,L-lactide, a Sustainable Amphiphilic Copolymer for Nano-Therapeutics*. Drug Delivery and Translational Research, 12(8), 1974-1990.
11. Fares, M.M., Salem, M.S., Khanfar, M., (2011). *Inulin and poly(acrylic acid) grafted inulin for dissolution enhancement and preliminary controlled release of poorly water-soluble Irbesartan drug*. International journal of pharmaceutics, 410(1-2), 206-211.

12. Janciauskaite, U., Makuska, R., (2009). *Cationic polyelectrolytes from natural building blocks of chitosan and inulin*. *Reactive and Functional Polymers*, 69(5), 300-305.
13. Siqueira, D. D., Luna, C.B.B., Araujo, E. M., Filho, E.A.D.S., Morais, D.D.D.S., Wellen, R.M.R., (2020). *Biodegradable Compounds of Poly (ϵ -Caprolactone) / Montmorillonite Clays*. *Materials Research*, 22.
14. Azimi, B., Nourpanah, P., Rabiee, M., Arbab, S., (2014). *Poly (ϵ -caprolactone) Fiber: An Overview*. *Journal of Engineered Fibers and Fabrics*, (9), Issue 3, 74.
15. ÖZSAĞIROĞLU, E., (2011). *Investigation Of Effects Of Reaction Mediums On Polycaprolactone Synthesis By Enzymatic Polymerization And Its Biodegradation*. Istanbul Technical University, Istanbul, Turkey.
16. Espinoza, S.M., Patil, H.I., Martinez, E.S.M., Pimentel, R.C., Ige, P.P., (2019). *Poly - ϵ -caprolactone (PCL), a promising polymer for pharmaceutical and biomedical applications: Focus on nanomedicine in cancer*. *International Journal of Polymeric Materials and Polymeric Biomaterials*, Taylor&Francis, 1,2.
17. Danafar, H., (2017). *Study of the Composition of Polycaprolactone /Poly (Ethylene Glycol) /Polycaprolactone Copolymer and Drug-to-Polymer Ratio on Drug Loading Efficiency of Curcumin to Nanoparticles*. *Jundishapur Journal of Natural Pharmaceutical Product*, (1), 12.
18. Yu, Z., Liu, L., (2007). *Biodegradable Poly(vinyl alcohol)-graft-poly(ϵ -caprolactone) Comp-like Polyester: Microwave Synthesis and Its Characterization*. *Journal of Applied Polymer Science*, 104(6), 3973-3979.
19. Hakemii, P., Ghadi, A., Mahjoub, S., Zabihi, E., Tashakkorian, H., (2021). *Fabrication of PCL-PEG-PCL nanocarrier for Co-loading of Docetaxel/Quercetin and assessment of its effect on growth inhibition of human liver cancer (Hep-G2) cell line*. *International Journal of Nano Dimension*, (4), 12.
20. Liu, C., Gong, C.Y., Pan, Y., Zhang, Y., Wang, J., Huang, M., Wang, Y., Wang, K., Gou, M., Tu, M., Wei, Y., Qian, Z., (2007). *Synthesis and characterization of a thermosensitive hydrogel based on biodegradable amphiphilic PCL-Pluronic (L35)-PCL block copolymers*. *Colloids and Surfaces A: Physicochemical and Engineering Aspects*, 302(1-3), 430-438.

21. Labet, M. and Thielemans, W., (2009). *Synthesis of polycaprolactone: a review*. Chemical Society Reviews, 38(12), 3484-3504.
22. Gotelli, G.A., Bonelli, P., Abraham, G.A., Sosnik, A., (2011). *Fast and Efficient Synthesis of High Molecular Weight Poly(epsilon-caprolactone) Diols by Microwave-Assisted Polymer Synthesis*. Journal of Applied Polymer Science, 121(3), 1321-1329.
23. Bai, X. And Mu, Z., (2019). *Research and Development of Microwave Irradiation Technology in Polymer Synthesis*. The 7th Annual International Conference on Materials Science and Engineering, Dalian, China.
24. Rahul, R., Sen, G., Jha, U., Mishra, S., (2014). *Carboxymethyl inulin:A novel flocculant for wastewater treatment*. International Journal of Biological Macromolecules, 63, 1-7.
25. Odrobinska, J. And Neugebauer, D., (2020). *Micellar Carriers Based on Amphiphilic PEG/PCL Graft Copolymers for Delivery of Active Substances*. Polymers, 12(12), 2876.
26. Mauro, N., Campora, C., Scialabba, C., Adamo, G., Licciardi, M., Ghersi, G., (2015). *Self-organized environment-sensitive inulin-doxorubici conjugate with a selective cytotoxic effect towards cancer cells*. Royal Society of Chemistry Advances, 5(41), 32421-32430.
27. Adams, M.L., Lavasanifar, A., Kwon, G.S., (2003). *Amphiphilic Block Copolymers for Drug Delivery*. Journal of pharmaceutical sciences, 92(7), 1343-1355.
28. Diao, Y.Y., Li, H.Y., Fu, Y.H., Han, M., Hu, Y.L., Jiang, H.L., Tsutsumi, Y., Wei, Q.C., Chen, D.W., Gao, J.Q., (2011). *Doxorubicin-loaded PEG-PCL copolymer micelles enhance cytotoxicity and intracellular accumulation of doxorubicin in adriamycin-resistant tumor cells*. International Journal of Nanomedicine, 1955-1962.
29. Yadav, S., Sharma, A.K., Kumar, P., (2020). *Nanoscale Self-Assembly for Therapeutic Delivery*. Frontiers in Bioengineering and Biotechnology, 8, 127.
30. Miao, Y., Qui, Y. Zhang, M., Yan, K., Zhang, P., Lu, S., Liu, Z., Shi, X., Zhao, X., (2020). *Aqueous Self-Assembly of Block Copolymers to Form Manganese Oxide-Based Polymeric Vesicles for Tumor Microenvironment-Activated Drug Delivery*. Nano-Micro Letters, 12, 1-15.
31. Qiu, Y., Zhu, Z., Miao, Y., Zhang, P., Jia, X., Liu, Z., Zhao, X., (2020). *Polymerization*

- of Dopamine Accompanying Its Coupling to Induce Self-Assembly of Block Copolymer and Application in Drug Delivery*. *Polymer Chemistry*, 11(16), 2811-2821.
32. Hu, Y., (2015). *Synthesis, self-assembly and controlled drug delivery of novel thermo-responsive and amphiphilic block copolymers based on polylactide, polyacrylamide and poly(oligo(ethylene glycol) methacrylate)*, Montpellier University, France.
 33. Xu, Q., Zhang, C., Cai, S., Zhu, P., Liu, L., (2010). *Large-scale microwave-assisted ring-opening polymerization of ϵ -caprolactone*. *Journal of Industrial and Engineering Chemistry*, 16(5), 872-875.
 34. Liao, L. Q., Liu, L. J., Zhang, C., He, F., Zhuo, R. X., Wan, K., (2002). *Microwave – Assisted ring-opening Polymerization of ϵ -caprolactone*. *Journal of polymer science*.
 35. Tan, Y., Cai, S., Liao, L., Wang, Q, Liu, L., (2009). *Microwave-assisted ring-opening polymerization of ϵ -caprolactone in presence of hydrogen phosphonates*. *The society of polymer science part A: Polymer Chemistry*, 40(11), 1749-1755.
 36. Kumari, A., Yadav, S. K. and Yadav, S. C., (2010). *Biodegradable polymeric nanoparticles based drug delivery systems*. *Colloids and surfaces B: biointerfaces*, 75(1), 1-18.
 37. Malam, Y., Loizidou, M. and Seifalian, A. M., (2009). *Liposomes and nanoparticles: nanosized vehicles for drug delivery in cancer*. *Trends in pharmacological sciences*, 30(11), 592-599.
 38. Peer, D., Karp, J. M., Hong, S., Farokhzad, O. C., Margalit, R. and Langer, R., (2020). *Nanocarriers as an emerging platform for cancer therapy*. *Nano-enabled medical applications*, 61-91.
 39. Yang, C., Merlin, D., (2019). *Nanoparticle-mediated drug delivery systems for the treatment of IBD: Current perspectives*. *International Journal of Nanomedicine*, 8875-8889.
 40. *BWH Crohn's & Colitis Center*, Brigham and women's hospital, <http://www.bwhcrohnscolitis.org/ibd-101/medications/5-asa/>(28.09.2022)
 41. *Sigma Aldrich, Merck*, 5-aminosalicylic acid (2022). <https://www.sigmaaldrich.com/TR/en/product/sigma/a3537>(30.09.2022)

42. *Wikipedia the free encyclopedia*, Mesalazine, (2022).
<https://en.wikipedia.org/wiki/Mesalazine>(03.10.2022)
43. NMR chemical shifts. https://web.pdx.edu/~lutzi/NMR_chmshfts.pdf(03.10.2022)
44. Kerman, I., Toppare, L., Yilmaz, F., Yagci, Y., (2005). *Thiophene ended ϵ -Caprolactone conducting copolymers and their electrochromic properties*. Journal of Macromolecular Science, Part A: Pure and Applied Chemistry, 42(4), 509-520.
45. Melanie, H., Susilowati, A., Iskandar, M., Lotulung, P., D., Andayani, D., G., S., (2015). *Characterization of inulin from local red dahlia (*Dahlia sp. L*) tubers by infrared spectroscopy*. Procedia Chemistry, 16, 78-84.
46. Elzein, T., Nasser-Eddine, M., Delaite, C., Bistac, S., Dumas, P., (2004). *FTIR study of polycaprolactone chain organization at interfaces*. Journal of colloid and interface science, 273(2), 381-387.
47. *Sigma Aldrich, Merck, IR spectrum table & chart*, (2022).
<https://www.sigmaaldrich.com/TR/en/technical-documents/technical-article/analytical-chemistry/photometry-and-reflectometry/ir-spectrum-table>(30.12.2022)
48. Barua, S., Mitragotri, S., (2014). *Challenges associated with penetration of nanoparticles across cell and tissue barriers: A review of current status and future prospects*. Nano today, 9(2), 223-243.
49. Clogston, J., D., Patri, A., K., (2011). *Zeta potential measurement*. Characterization of nanoparticles intended for drug delivery, 63-70.
50. Honary, S., Zahir, F., (2013). *Effect of zeta potential on the properties of nano-drug delivery systems-A Review (Part 2)*. Tropical journal of pharmaceutical research, 12(2), 265-273.
51. Afinjuomo, F., Fouladian, P., Barclay, T., G., Song, Y., Petrovsky, N., Garg, S., (2020). *Influence of oxidation degree on the physicochemical properties of oxidized inulin*. Polymers, 12(5), 1025.
52. Rusu, M., Ursu, M., (2006). *Poly(vinyl chloride) and Poly(ϵ -caprooverlactone) blends for medical use*. Journal of Thermoplastic Composite Materials, 19(2), 173-190.
53. Bruschi, M. L., (2015). *Mathematical models of drug release*. Strategies to modify the

drug release from pharmaceutical systems, 63, 63-86.

54. Paarakh, M., P., Jose, P., A., Setty, C., Peter, D.,V., (2018). *Release kinetics-concepts and applications*. International journal of pharmacy and technology. 8(1), 12-20.
55. Scientific, Thermo Fisher, (2016). *Carbodiimide crosslinker chemistry*. *Piercenet.com/browse*. Cfm.
56. *Chemistry Steps*, Amides from Carboxylic Acids-DCC and EDC Coupling, <https://www.chemistrysteps.com/amides-from-carboxylic-acids-dcc-edc-coupling/> (27.02.2023)
57. Hermanson, G., T., (2013). *Bioconjugate techniques*. Academic press.